NACA TM 1317

NATIONAL ADVISORY COMMITTEE FOR AERONAUTICS

TECHNICAL MEMORANDUM 1317

58

A SIMPLE NUMERICAL METHOD FOR THE CALCULATION OF THE LAMINAR BOUNDARY LAYER

By K. Schröder

Translation of ZWB Forschungsbericht Nr. 1741, February 25, 1943

NACA

Washington
April 1952

ERRATA NO. 1

NACA TM 1317

A SIMPLE NUMERICAL METHOD FOR THE CALCULATION OF THE LAMINAR BOUNDARY LAYER

By K. Schröder

April 1952

Every effort is made by the NACA to insure that its published translations are accurate reproductions of the original work of the authors. Papers are selected for translation on the basis of interest and probable usefulness and, although an examination is made for technical soundness, the Committee cannot assume responsibility for the accuracy of the detailed results presented by the author in the original paper. The Committee will, of course, call attention to any errors observed at the time of the publication or subsequent thereto.

A recent application of equation 21 on page 14 of TM 1317 indicated that the denominator of the last term, which is given as 2 in the NACA translation and in the original German document, should be l.

C. 1

ERRATA NO. 2

NACA TM 1317

A SIMPLE NUMERICAL METHOD FOR THE CALCULATION OF
THE LAMINAR BOUNDARY LAYER
By K. Schröder

April 1952

In the errata no. 1 issued on this paper, the last term of equation (21) was corrected as follows:

$$\frac{\overline{U}(\xi_{\rho+1}) - \overline{U}(\xi_{\rho-1})}{l}$$

Subsequent consideration of this errata indicates that this corrected term is valid only for the case when $k = \frac{l^2}{2}$. Therefore, when equation (21) is used for general applications, the last term therein should be

$$l \frac{\overline{U}(\xi_{\rho+1}) - \overline{U}(\xi_{\rho-1})}{2k}$$

NACA-Langley - 8-20-53 - 1000

NATIONAL ADVISORY COMMITTEE FOR AERONAUTICS

TECHNICAL MEMORANDUM 1317

A SIMPLE NUMERICAL METHOD FOR THE CALCULATION OF THE LAMINAR BOUNDARY LAYER*

By K. Schröder

ABSTRACT

A method is described which permits an arbitrarily accurate calculation of the laminar boundary layer with the aid of a difference calculation. The advantage of this method is twofold. Starting from Prandtl's boundary-layer equation and the natural boundary conditions, nothing needs to be neglected or assumed, and not too much time is required for the calculation of a boundary-layer profile development. So far, the method has been tested successfully in the continuation of the Blasius profile on the flat plate, on the circular cylinder investigated by Hiemenz, and on an elliptical cylinder of fineness ratio 1:4. Above all, this method offers for the first time a possibility of control by comparison of methods known so far, all of which are burdened with more or less decisive presuppositions.

OUTLINE

---

*"Ein einfaches numerisches Verfahren zur Berechnung der laminaren Grenzschicht." Zentrale für wissenschaftliches Berichtswesen der Luftfahrtforschung des Generalluftzeugmeisters (ZWB) Forschungsbericht Nr. 1741, Berlin-Adlershof, February 25, 1943.

I. INTRODUCTION

The flow processes in the laminar boundary layer may be described by Prandtl's boundary-layer equation. If one limits oneself to the two-dimensional steady case and introduces, in a suitable region around a profile contour C situated in a flow, a curvilinear coordinate system s,n, the coordinate lines of which consist of parallel curves and normals of C, that equation reads

$$v_s \frac{\partial v_s}{\partial s} + v_n \frac{\partial v_s}{\partial n} + p'(s) = \frac{1}{R} \frac{\partial^2 v_s}{\partial n^2} \tag{1}$$

when v_s, v_n signify the velocity components in the s,n system, R the Reynolds number, and $p = p(s)$ the pressure distribution along C taken from a measurement or calculation[1]. Equation (1) is complemented by the continuity equation

$$\frac{\partial v_s}{\partial s} + \frac{\partial v_n}{\partial n} = 0 \tag{2}$$

The transformation

$$\eta = n\sqrt{R} \qquad v_\eta = v_n \sqrt{R}$$

yields, instead of equations (1) and (2), the equation system

$$v_s \frac{\partial v_s}{\partial s} + v_\eta \frac{\partial v_s}{\partial \eta} + p'(s) = \frac{\partial^2 v_s}{\partial \eta^2} \tag{3}$$

$$\frac{\partial v_s}{\partial s} + \frac{\partial v_\eta}{\partial \eta} = 0 \tag{4}$$

in which R no longer appears explicitly.

---

[1]A mathematically complete derivation of equations (1) and (2) based on physically plausible assumptions may be found in H. Schmidt's and K. Schröder's report entitled "Die Prandtlsche Grenzschichtgleichung als asymptotische Näherung der Navier-Stokesschen Differentialgleichungen bei unbegrenzt wachsender Reynoldsscher Kennzahl" (Prandtl's boundary-layer equation as an asymptotic approximation of Navier-Stokes' differential equations for indefinitely increasing Reynolds number) Deutsche Mathematik, 6, Heft 4/5, pp. 307-322. A survey of related literature is given in H. Schmidt's and K. Schröder's report "Laminare Grenzschichten, I. Teil" (Laminar boundary layers, part I) Luftfahrtforschung 19, Lieferung 3, 1942.

The following boundary conditions for the integration of equations (3) and (4) are usually selected in boundary-layer theory as the natural ones from the physical point of view. For an initial value $s = s_0$ an entrance profile

$$v_s = v_s(s_0,\eta)$$

is prescribed as a function of η (entrance condition). Furthermore, in consequence of the adherence of the fluid to the contour, the relations

$$\left[v_s\right]_0 = 0 \qquad \left[v_\eta\right]_0 = 0$$

which are to be interpreted as limiting processes, are to be valid along C (adherence condition). Finally, for s-values larger than or equal to s_0 the velocity component v_s is to converge for $\eta \longrightarrow \infty$ toward the velocity $U(s)$ which is connected with the prescribed pressure distribution $p(s)$ by

$$U(s)\, U'(s) = - p'(s) \tag{5}$$

(transitional condition).

The general significance of these boundary conditions will be discussed more thoroughly in the second part of the Luftfahrtforschung report quoted in footnote 1. Here we shall only point out that the transitional condition formulated for $\eta \longrightarrow \infty$ must not be confused with a condition for $n \longrightarrow \infty$ since for the latter limiting process the velocity components converge toward those of the basic flow[2]. The limiting process $\eta \longrightarrow \infty$ denotes, on the contrary, the asymptotic transition to the boundary values, resulting along $\underline{C}$ of the outer potential flow obtained for $R \longrightarrow \infty$. This can best be made clear by the example of the stagnation-point flow at the flat plate, treated in the second report indicated in footnote 1 (by the author and H. Schmidt). Whereas the quantity δ there specified as boundary-layer thickness tends like $1/\sqrt{R}$ toward zero, a quantity d tending toward zero, for instance, like $1/\sqrt[4]{R}$, can be prescribed in such a manner that the flow outside of a layer of the thickness d adhering to the contour for $R \longrightarrow \infty$ converges toward the outer potential flow. However, to the asymptotic transition toward the boundary values of this assumed potential

---

[2]It is assumed, of course, that this limiting process is meaningful.

flow along C then there corresponds the limiting process

$$\lim_{R \to \infty} \eta_d = \lim_{R \to \infty} d\sqrt{R} = \infty$$

So far, an appropriate existence and uniqueness theorem for this boundary-value problem does not exist. However, the results obtained with the new method described below show that the statement of the problem is perfectly sensible.

In the literature it has been pointed out more than once[3] that formal power series developments of the function representing the solution with respect to η make the fact plausible that the entrance profile cannot be selected completely arbitrarily, but that it is dependent on the pressure distribution $p = p(s)$.

Our method for the determination of the velocity profiles yields a numerical solution of the mentioned boundary-value problem with the aid of the difference calculation; it is superior to other methods because it requires no assumptions beyond equations (3) and (4) and the boundary conditions. In our method, the boundary-layer bonds of the entrance profile do not appear directly and thus do not cause any difficulties in the numerical calculation. A severe violation of these bonds causes, in our method, the variation of the successive boundary-layer profiles to become completely disordered. Small violations of these bonds, in contrast, do not exert any considerable effect on the further development of the profile[4].

---

[3]Compare S. Goldstein "Concerning Some Solutions of the Boundary-Layer Equations in Hydrodynamics," Proc. Cambridge Phil. Soc. 26, 1930, pp. 1-30, L. Prandtl, "Zur Berechnung der Grenzschichten" (Concerning Calculation of the Boundary Layers) ZAMM. 18, 1938, pp. 77-82, (NACA TM 959) and H. Görtler, "Weiterentwicklung eines Grenzschichtprofils bei gegebenem Druckverlauf" (Further development of a boundary-layer profile for prescribed pressure variation) ZAMM. 19, 1939, pp. 129-140.

[4]L. Prandtl and H. Görtler (reports quoted in footnote 3) arrive at the same conclusion, although on another basis.

II. GENERAL REPRESENTATION OF THE METHOD

If one introduces into equation (3), instead of s, the new independent variable

$$\xi = \int_{s_0}^{s} \frac{dt}{U(t)} \tag{6}$$

under the assumption that $U(s) \neq 0$ for $s \geqq s_0$ whereby

$$\frac{d\xi}{ds} = \frac{1}{U(s)}$$

is valid, and if one uses the new designations

$$u(\xi,\eta) = v_s(s,\eta),\ \overline{U}(\xi) = U(s(\xi)),\ u^*(\xi,\eta) = u(\xi,\eta) - \overline{U}(\xi)$$

there follows from equations (3) and (4) by way of

$$v_\eta = -\frac{1}{\overline{U}(\xi)} \int_0^\eta \frac{\partial u}{\partial \xi}\, d\eta$$

with equation (5) taken into consideration, our initial equation

$$\frac{\partial u^*}{\partial \xi} - \frac{\partial^2 u^*}{\partial \eta^2} = \frac{1}{\overline{U}(\xi)} \frac{\partial u}{\partial \eta} \int_0^\eta \frac{\partial u}{\partial \xi}\, d\eta - \frac{u^*}{\overline{U}(\xi)} \frac{\partial u}{\partial \xi} \tag{7}$$

According to the statement of the problem in the introduction, we have to find a solution

$$u^* = u^*(\xi,\eta)$$

of equation (7) for all points (ξ,η) in the right upper quadrant of the plane of the rectangular Cartesian ξ,η coordinates[5] which in approaching the straight lines

$$\xi = 0 \quad \text{or} \quad \eta = 0 \quad \text{respectively}$$

---

[5]If separation phenomena appear, the solution will, in general, be of interest only up to the separation point or possibly a little way beyond it.

tends toward prescribed functions:

$$\lim_{\xi \to 0} u^*(\xi,\eta) = v_s(s_o,\eta) - U(s_o) \qquad (\eta \geqq 0) \tag{8}$$

or

$$\lim_{\eta \to 0} u^*(\xi,\eta) = -\overline{U}(\xi) \qquad (\xi \geqq 0) \tag{9}$$

and which vanishes for $\eta \to \infty$

$$\lim_{\eta \to \infty} u^*(\xi,\eta) = 0 \qquad (\xi \geqq 0) \tag{10}$$

The fundamental formulation of our method consists in using the functional relation (7) - in the sense of the known method of successive approximations - for the calculation from a prescribed approximate solution which already satisfies the indicated boundary conditions of a sequence of corrected functions which converges toward the actual solution of the problem; one substitutes the last obtained approximate solution every time on the left side of equation (7) and integrates the resulting partial differential equation of the type of the inhomogeneous heat conduction equation.

The examples so far calculated numerically showed that the iteration process is obviously convergent. Nevertheless, a general proof of this fact would be very desirable and we reserve returning, in a given case, to a mathematical examination of these problems. (Compare also Section V.)

One may characterize the method by stating as the desired result a continual improvement of a given approximate solution in the sense of Oseen's method of linearization. Then this linearization of the hydrodynamic equations of motion (which, of course, for the boundary-layer flow taken by itself is not permissible) consists in introducing the velocity loss u^* and in neglecting all nonlinear terms in u^*,v and their derivatives. From equation (3) one would thereby obtain

$$U(s)\frac{\partial u^*}{\partial s} - \frac{\partial^2 u}{\partial \eta^2} + u^*\frac{dU}{ds} = 0$$

thus on the left side (aside from the term $u^*\frac{dU}{ds}$ which, however, does not alter the character of the equation) precisely the expression which also appears on the left side of our initial equation (7).

In integrating (under the boundary conditions (8), (9), and (10)) the differential equation

$$\frac{\partial u^*}{\partial \xi} - \frac{\partial^2 u^*}{\partial \eta^2} = f(\xi,\eta) \tag{11}$$

into which had been introduced for abbreviation the function

$$f(\xi,\eta) = \frac{1}{\overline{U}(\xi)} \frac{\partial u}{\partial \eta} \int_0^{\eta} \frac{\partial u}{\partial \xi} \, d\eta - \frac{u^*}{\overline{U}(\xi)} \frac{\partial u}{\partial \xi} \tag{12}$$

to be regarded as known in the sense of our approximations, one may now use successfully the difference calculation. For the homogeneous equation this has been done, simultaneously with a proof of convergence, by R. Courant, K. Friedrichs, and H. Lewy[6]. For the inhomogeneous equation here dealt with, the proof of convergence together with a formula for error estimation may be found in a paper by L. Collatz[7].

If one covers the right upper quadrant of the ξ,η plane by a net of lattice points with the coordinates

$$\xi_\rho = \rho k \qquad \eta_\sigma = \sigma l \qquad (\rho,\sigma \geqq 0, \text{ integers})$$

(compare fig. 1) and introduces at the same time, with a view to later applications, the new designations

$$u_{\rho,\sigma} = u(\xi_\rho,\eta_\sigma), \; u^*_{\rho,\sigma} = u^*(\xi_\rho,\eta_\sigma)$$

$$\left[\frac{\partial u}{\partial \xi}\right]_{\xi=\xi_\rho,\eta=\eta_\sigma} = \left[\frac{\partial u}{\partial \xi}\right]_{\rho,\sigma} \quad \left[\frac{\partial u}{\partial \eta}\right]_{\xi=\xi_\rho,\eta=\eta_\sigma} = \left[\frac{\partial u}{\partial \eta}\right]_{\rho,\sigma}$$

---

[6] R. Courant, K. Friedrichs, and H. Lewy: "Über die partiellen Differenzengleichungen der mathematischen Physik" (On the partial difference equations of mathematical physics), Math. Ann. 100, 1928, pp. 32-74, particularly pp. 47-52.

[7] L. Collatz: "Das Differenzenverfahren mit höherer Approximation für lineare Differenzengleichungen" (The difference method with higher approximation for linear difference equations), Schriften des Math. Sem. u.d. Inst. f. agewandte Math.d.Univ. Berlin, Bd. 3, Heft 1, 1935.

there corresponds to the differential equation (11) the difference equation of first approximation

$$\frac{u^*_{\rho+1,\sigma} - u^*_{\rho,\sigma}}{k} - \frac{u^*_{\rho,\sigma+1} - 2u^*_{\rho,\sigma} + u^*_{\rho,\sigma-1}}{l^2} = f_{\rho,\sigma} \tag{13}$$

If one selects the step magnitudes k and l in ξ and η direction not independent of each other but so that

$$k = \frac{l^2}{2} \tag{14}$$

equation (13) is transformed into the simpler difference equation

$$u^*_{\rho+1,\sigma} = \frac{u^*_{\rho,\sigma+1} + u^*_{\rho,\sigma-1}}{2} + kf_{\rho,\sigma} \tag{15}$$

It can be shown that the solution of equation (15) for the corresponding boundary-value problem for $l \longrightarrow 0$ and therewith also for $k \longrightarrow 0$ converges toward the known solution of the boundary value problem of equation (11).

Since the values

$$u^*_{\rho,0} \; (\rho \geqq 0) \qquad u^*_{0,\sigma} \; (\sigma \geqq 0) \qquad f_{\rho,\sigma} \; (\rho \geqq 0, \sigma \geqq 0)$$

are known, one may, according to equation (15), successively calculate all values

$$u^*_{\rho,\sigma} \qquad (\rho \geqq 0, \sigma \geqq 0)$$

progressing stepwise from lattice point column to lattice point column.

Actually, however, we apply another correction at every step in order to compensate the systematic error originating by the fact that the derivative appearing on the left side of equation (11)

$$\left[\frac{\partial u^*}{\partial \xi}\right]_{\rho,\sigma}$$

was replaced by the difference quotient of first approximation

$$\frac{u^*_{\rho+1,\sigma} - u^*_{\rho,\sigma}}{k}$$

(Compare the following section.)

One notes that due to the transitional condition (10) for the entrance profile $u^*_{0,\sigma}$ necessarily must vanish for $\sigma \longrightarrow \infty$ and that $f_{\rho,\sigma}$ likewise vanishes for $\sigma \longrightarrow \infty$, since even the approximate solution used for the formation of $f_{\rho,\sigma}$ was supposed to satisfy the condition (10); hence one recognizes that the corrected solution (obtained with the aid of the difference calculation in the manner described above) also satisfies the transitional condition (10).

III. PRACTICAL EXECUTION

In practice one may vary the method in such a manner that one does not at all require an approximate solution prescribed at the outset in the first quadrant of the ξ,η-plane; one rather determines this approximate solution for every step and then improves it to the desired accuracy before passing on to the next step. Thus one applies a combined system of continuation and correction.

If one deals with the flow about a profile contour, the initial profile at the point $s = s_0$ is best taken from the well-known power-series developments by Blasius-Hiemenz, the coefficients of which for the first three terms were given in table form by Howarth[8]. For reasons of convergence, these broken-off series will represent a good approximation of the solution of the boundary-layer equation only at a small distance from the forward stagnation point $(s = 0)$ of the outer potential flow. In the permissible range they represent, as it were, an improved stagnation point flow.

Our calculations so far have shown that the series are serviceable up to s-values for which the "first boundary layer bond"

$$\left[\frac{\partial^2 v_s}{\partial \eta^2}\right]_{\eta=0} = p'(s) = -\frac{d\overline{U}(\xi)}{d\xi} \tag{16}$$

[8]Compare L. Howarth: On the calculation of steady flow in the boundary layer near the surface of a cylinder in a stream. R & M no. 1632, 1934.

which is a direct result of equations (3) and (6) is satisfied with sufficient accuracy.

In practice, one has therefore to start the calculation by approximating the function U(s) for small s-values as well as possible by a polynomial of the form

$$U(s) = u_1 s + u_3 s^3 + u_5 s^5$$

for the case of a profile symmetrical in free-stream direction, or respectively, of the form

$$U(s) = u_1 s + u_2 s^2 + u_3 s^3$$

for the case of a profile unsymmetrical in free-stream direction; one may sometimes get by with only two terms.

After having determined, in the manner described above, the value $s_o > 0$ at which the continuation method may start, one first sets up the connection (given by equation (6))

$$\xi = \int_{s_o}^{s} \frac{dt}{U(t)} \qquad (s > s_o)$$

by evaluating the integral on the right side, for instance according to the trapezoidal rule. One graphically represents the functions $\xi = \xi(s)$ and $U = U(s)$ in a common diagram so that $\overline{U} = \overline{U}(\xi)$ can be immediately taken from it.

The step magnitudes k and l, connected by equation (14), must be selected so that, first, a sufficient number of subdivision points are distributed over the profiles to be calculated, and second, a sufficiently rapid continuation in ξ direction is possible. When profiles of not too pronounced S-shape (near the separation point) are to be calculated, eight to ten equidistant subdivision points generally will be sufficient to define the profile. In upward direction (that is, for large η values) one will have to take so many subdivision points that the profile dies out sufficiently gradually toward the asymptotic value $\overline{U}$. This provides a first indication for the selection of l and therewith also of k. It should finally be remarked regarding the step magnitude k that it must be at least large enough to make, for fixed ξ and variable η, the derivatives $\frac{\partial u}{\partial \xi}$ (obtained in first approximation by formation of difference quotients) take a reasonably regular course (compare the following discussion). Hence the lower limit is set for k and therewith also for l.

On the other hand, one will be forced to choose the smallest possible step magnitude k at points ξ where the curves $u = u(\xi, \text{const})$ exhibit great curvatures (which occurs particularly directly ahead of the separation point), in order to make a sufficiently exact calculation of the profiles possible. There l, too, will necessarily be small. Since, however, the boundary-layer thickness has greatly increased at the separation point, one will have there a great many subdivision points distributed over the profile. This is in one respect convenient - the position of the separation point is better defined. On the other hand, the expenditure of work increases at such points. However, at the end of this section we shall point out a possibility of reducing the steps in ξ direction without necessarily having to accept a step reduction in η direction. At the same time we shall then be able to indicate a criterion by which the necessity of a step reduction in ξ direction may be recognized.

Once a certain selection of step magnitudes has been decided upon, it is a question of obtaining a first approximation for the values $f_{0,\sigma}$ appearing in equation (15), in order to be able to execute the first step in ξ direction. It should be noted that together with the initial profile at $s = s_0$ also the values of u for values $s < s_0$ may be taken from the series developments. Particularly the values $u_{-1,\sigma}$ (that is, the profile one step ahead of the initial profile) are thus known.

We then put for a first approximation of the $\left[\frac{\partial u}{\partial \xi}\right]_{0,\sigma}$ occuring in $f_{0,\sigma}$:

$$\left[\frac{\partial u}{\partial \xi}\right]_{0,\sigma} = \frac{u_{0,\sigma} - u_{-1,\sigma}}{k}$$

Therewith $\int_0^\eta \left[\frac{\partial u}{\partial \xi}\right] d\eta$ too can be evaluated numerically. Our calculation experience has shown that this integration may be very conveniently carried out with sufficient accuracy by use of the trapezoidal rule with the aid of the present subdivision; this can be done purely schematically by calculation according to tables. For at the ξ points where the derivatives $\frac{\partial u}{\partial \xi}$ become very large - whereby the values $\int_0^\eta \frac{\partial u}{\partial \xi} d\eta$ come to be of great importance in the calculation of the profiles and must be determined relatively exactly as for instance in the neighborhood of the separation point - it will be necessary to select small k (and therewith also l) values so that a sufficient number of subdivision points are distributed over the profile to allow application of the trapezoidal rule with sufficient accuracy.

If one puts, furthermore, with good approximation

$$\left[\frac{\partial u}{\partial \eta}\right]_{0,\sigma} = \frac{u_{0,\sigma+1} - u_{0,\sigma-1}}{2l} \tag{17}$$

$u^*_{1,\sigma}$ and $u_{1,\sigma}$ may be calculated in first approximation.

The values thus obtained will be denoted by $\left[u^*_1\right]_{1,\sigma}$ and $\left[u_1\right]_{1,\sigma}$. It will be best to arrange the entire calculation procedure in the form of a table (compare table I on page 31). With the values obtained $\left[u_1\right]_{1,\sigma}$ one will form corrected values of the derivatives $\left[\frac{\partial u}{\partial \xi}\right]_{0,\sigma}$ according to the scheme

$$\left[\frac{\partial u_1}{\partial \xi}\right]_{0,\sigma} = \frac{\left[u_1\right]_{1,\sigma} - u_{-1,\sigma}}{2k}$$

whereupon one obtains (with the aid of table II on page 31) a second approximation $\left[u_2\right]_{1,\sigma}$ for the values $u_{1,\sigma}$ with the values $\gamma_\sigma, \epsilon_\sigma$, and C_σ taken from the first table. Whereas the derivatives $\left[\frac{\partial u}{\partial \xi}\right]_{0,\sigma}$ formed in first approximation might show at a few points σ an irregular course, this will generally no longer be the case for the corrected derivatives $\left[\frac{\partial u}{\partial \xi}\right]_{0,\sigma}$. The columns for the quantities D_σ, $\left[\bar{u}^*_2\right]_{1,\sigma}$ and $\left[\bar{u}_2\right]_{1,\sigma}$ occurring further on in table II will be explained only later.

This procedure is continued until the values obtained in the third-from-last column of the table no longer vary in the desired decimal. In the examples we calculated the iteration was carried so far that for every step ξ_σ the values $u_{\rho,\sigma}$ no longer varied except for an error of about 1/4 to 1/2 percent of the maximum velocity $\bar{U}(\xi_\rho)$ in each case. For the selected step magnitude k this was the case after two to three iterations.

Due to the favorable position of the errors, the profiles calculated in the manner described generally show a very smooth course. If the $u = u(\xi,\text{const})$ are concave in respect to the ξ axis, as is the case for instance in the flow about the circular cylinder or the ellipse near the separation point (compare fig. 7 and fig. 12), the convergence occurs only on one side in the direction from larger to smaller values for u. The opposite behavior exists when the course of this curve is convex with respect to the ξ axis as is the case for instance in the boundary-layer flow at the flat plate.

If one wants to obtain with the described procedure a calculation of the u variation as accurate as possible without selecting too small a step magnitude k, thereby increasing too much the expenditure in calculation, one will find it necessary (as mentioned before) to make at every step a correction which takes the fact into account that in setting up the basic equation (15) the difference quotient of first approximation only was substituted for the derivative $\left[\frac{\partial u^*}{\partial \xi}\right]_{\rho,\sigma}$

If one were to select instead the representation of higher approximation

$$\left[\frac{\partial u^*}{\partial \xi}\right]_{\rho,\sigma} = \frac{u^*_{\rho+1,\sigma} - u^*_{\rho-1,\sigma}}{2k}$$

one would obtain by maintaining equation (14)

$$u^*_{\rho+1,\sigma} = u^*_{\rho-1,\sigma} + u^*_{\rho,\sigma+1} + u^*_{\rho,\sigma-1} - 2u^*_{\rho,\sigma} + 2kf_{\rho,\sigma} \tag{18}$$

instead of equation (15).

Since this relation, however, (as can be seen immediately) behaves considerably less favorably regarding propagation of errors than equation (15), the profiles calculated with its aid will no longer show the smooth course mentioned before. Calculation practice has shown that one obtains very smooth curves if one writes instead of equation (18)

$$u^*_{\rho+1,\sigma} = u^*_{\rho-1,\sigma} + 2k\left[\frac{\partial^2 u^*}{\partial \eta^2}\right]_{\rho,\sigma} + 2kf_{\rho,\sigma} \tag{19}$$

and forms the second derivative appearing in it according to the scheme

$$\left[\frac{\partial^2 u^*}{\partial \eta^2}\right]_{\rho,\sigma} = \frac{\left[\frac{\partial u}{\partial \eta}\right]_{\rho,\sigma+1} - \left[\frac{\partial u}{\partial \eta}\right]_{\rho,\sigma-1}}{2l} \tag{20}$$

from the first derivative $\left[\frac{\partial u}{\partial \eta}\right]_{\rho,\sigma}$ already calculated in good approximation according to equation (17) by jumping over. However, the case $\sigma = 1$

requires special consideration since $\left[\frac{\partial u}{\partial \eta}\right]_{\rho,0}$ is not known at first. But if one takes into consideration that according to equation (16)

$$\left[\frac{\partial^2 u}{\partial \eta^2}\right]_{\rho,0} = -\frac{d\overline{U}(\xi_\rho)}{d\xi}$$

one may put

$$\begin{aligned}\left[\frac{\partial u}{\partial \eta}\right]_{\rho,0} &= \left[\frac{\partial u}{\partial \eta}\right]_{\rho,1} - l\left[\frac{\partial^2 u}{\partial \eta^2}\right]_{\rho,0} \\ &= \left[\frac{\partial u}{\partial \eta}\right]_{\rho,1} + l\,\frac{d\overline{U}(\xi_\rho)}{d\xi} = \left[\frac{\partial u}{\partial \eta}\right]_{\rho,1} + l\,\frac{\overline{U}(\xi_{\rho+1}) - \overline{U}(\xi_{\rho-1})}{2k}\end{aligned} \tag{21}$$

and hence calculate the value on the left from $\left[\frac{\partial u}{\partial \eta}\right]_{\rho,1}$ already known according to equation (17).

We now use the relation (19) not as a substitute for (15) in the sense that the entire calculation is to be made with (19), for it became clear - particularly near the separation point where the derivatives $\frac{\partial u}{\partial \xi}$ become very large - that the convergence relations here can be easily blurred (unless an especially small k value was selected); the values $u_{\rho,\sigma}$ obtained by iteration do not remain quite fixed, but creep on continously, although only by small amounts (compare also the remarks in section V).

Rather we use equation (19) for making a correction in the values $u_{1,\sigma}$ obtained after the last iteration in the manner described above. With the aid of the value $\left[\frac{\partial u}{\partial \eta}\right]_{0,\sigma}$ $(\sigma \geqq 1)$, (already contained in the fourth column of table I) to which we add the value $\left[\frac{\partial u}{\partial \eta}\right]_{0,0}$ just calculated according to equation (21) we determine (taking equations (20) and (14) into consideration) the values

$$D_\sigma = u^*_{-1,\sigma} + 2k\left[\frac{\partial^2 u}{\partial \eta^2}\right]_{0,\sigma} = u^*_{-1,\sigma} + \frac{l}{2}\left(\left[\frac{\partial u}{\partial \eta}\right]_{0,\sigma+1} - \left[\frac{\partial u}{\partial \eta}\right]_{0,\sigma-1}\right).$$

We now assume, for instance, that the values $\left[u_2\right]_{1,\sigma}$ prescribed by table II were the final values even in the first procedure; we then insert the values D_σ in table II and calculate with the quantities $A_\sigma + B_\sigma$ appearing in them the values (corrected with respect to $\left[u^*_2\right]_{1,\sigma}$

$$\left[\bar{u}^*_2\right]_{1,\sigma} = D_\sigma + 2(A_\sigma + B_\sigma)$$

these values, too, we note in the table. In the last column of this table we write the values

$$\left[\bar{u}_2\right]_{1,\sigma} = \bar{U}(\xi_1) + \left[\bar{u}^*_2\right]_{1,\sigma}$$

If the corrected values $\left[\bar{u}_2\right]_{1,\sigma}$ deviate too much (that is, by more than 1/4 to 1/2 percent of $\bar{U}$) from $\left[u_2\right]_{1,\sigma}$ we calculate with the derivatives

$$\left[\frac{\partial u_2}{\partial \xi}\right]_{0,\sigma} = \frac{\left[\bar{u}_2\right]_{1,\sigma} - \left[u\right]_{-1,\sigma}}{2k}$$

once more corrected values according to table III, p.31. The values $\left[\bar{u}_3\right]_{1,\sigma}$ then represent the final values for the profile at the point $\xi = \xi_1$.

For calculation of every step in ξ direction one must, therefore, calculate three to four of the calculation tables mentioned. The time expenditure may be estimated at approximately three to four hours per step. It should be stressed that all calculation operations are of purely schematic character and can therefore readily be performed by assistants.

The values obtained are plotted on millimeter graph paper and the curve drawn through them. If slight scatter has resulted, after all, at one point or the other, one eliminates it with the aid of the drawing before starting on the next step.

If the graph of the profile calculated just now shows that the curve, due to the increase in boundary-layer thickness, at the upper end no longer dies out gradually enough toward the asymptotic value $\bar{U}$, one adds, in calculating the following step, and η subdivision point in upward direction.

The following condition should be mentioned which became evident in the practical calculation. If a step magnitude not sufficiently small is selected, two successive profiles may, due to accumulation of errors, show points where they are somewhat too close, or else somewhat too distant from each other, compared to their actual course. In the calculation this can be recognized by the fact that the third profile following these two profiles shows a behavior, at these points, compared to the second profile opposite to the behavior of the first compared to the second profile. For η values at which the first two profiles were too close one notices a gap somewhat too wide between the last two and vice versa. If one does not want to repeat the calculation with smaller steps, one may, as was found practically to be useful, once omit the corrective calculation mentioned before for the profile to be calculated next, thereby eliminating the fluctuating of the profiles, and may then continue calculating in the normal manner.

According to our calculation experiences one can recognize that the step magnitude k must be reduced in ξ direction by the fact that the two $\bar{u}$ values obtained in the corrective calculation which pertain to the same η_σ (thus in the example considered above the values $\left[\bar{u}_2\right]_{1,\sigma}$ and $\left[\bar{u}_3\right]_{1,\sigma}$) deviate from each other by considerably more than 1/4 to 1/2 percent of the pertaining $\bar{U}$ value.

If a new step magnitude in the ξ direction, k_1, is selected $k_1 < k$ $\left(\text{for instance, } k_1 = \frac{k}{2}\right)$ there appears as a result, because of equation (14), also a new step magnitude.

$$l_1 = \sqrt{2k_1}$$

in η direction. If one wants to continue the calculation with the smaller steps k_1 for instance starting from $\xi = \xi_r$ one needs as the initial values for further calculation the numbers

$$u(\xi_r, \sigma l_1) \qquad u(\xi_r - k_1, \sigma l_1) \qquad (\sigma = 1, 2, \ldots)$$

The first named numbers may be read off directly on the profile curve for $\xi = \xi_r$ already obtained. In order to obtain the latter, a double graphic interpolation must be made. One plots versus ξ the values

$u\left(\xi_\rho, \sigma l_1\right)$ $(\sigma = 1,2 \ldots)$ read off for the values of $\xi = \xi_\rho\left(\rho \leqq r\right)$ from the curves of the previously calculated profiles. Generally it will be sufficient to do this for the values $u\left(\xi_\rho, \sigma l_1\right)$ of three successive profiles, thus for $\rho = r - 2, r - 1, r$. From the curves drawn through them $u = u(\xi, \sigma l_1)$ $(\sigma = 1,2 \ldots)$ one may then read off the values $u\left(\xi_r - k_1, \sigma l_1\right)$ $(\sigma = 1,2 \ldots)$.

If a boundary layer is to be calculated up to the separation point, it will in general be necessary to select, in the proximity of the separation point, rather small steps k. Since, however, due to the large increase in boundary-layer thickness, the profiles are here very elongated, one would obtain, because of the small step magnitude l in η direction, a very great number of subdivision points over the profile; this would of course increase the time expenditure for the calculation of a step. However, one may save a great deal of calculation expenditure by selecting, instead of equation (7), for instance

$$\frac{1}{2}\frac{\partial u^*}{\partial \xi} - \frac{\partial^2 u^*}{\partial \eta^2} = \frac{1}{\overline{U}(\xi)}\frac{\partial u}{\partial \eta}\int_0^\eta \frac{\partial u}{\partial \xi}\,d\eta - \left(\frac{u^*}{\overline{U}(\xi)} + \frac{1}{2}\right)\frac{\partial u}{\partial \xi} + \frac{1}{2}\frac{d\overline{U}(\xi)}{d\xi} \tag{22}$$

as the initial equation, and then performing the integration as before. If one again denotes the step magnitudes in ξ direction by k, those in η direction by l, one obtains instead of equation (14) the relation

$$k = \frac{l^2}{4}$$

To the same l as in the first considered case, therefore, there corresponds half the step magnitude in ξ-direction.

In this manner the step reductions were carried out for the following examples of boundary-layer flow on the circular and elliptic cylinder. The convergence of the iterations now occurred no longer only on one side toward the limit but alternately (except for the values assumed for small η_σ.

The numerical calculation showed further that a further step reduction in ξ direction, still for the same l, for instance with the aid of the initial relation

$$\frac{1}{4}\frac{\partial u^*}{\partial \xi} - \frac{\partial^2 u^*}{\partial \eta^2} = \frac{1}{\overline{U}(\xi)}\frac{\partial u}{\partial \eta}\int_0^\eta \frac{\partial u}{\partial \xi}\,d\eta - \left(\frac{u^*}{\overline{U}(\xi)} + \frac{3}{4}\right)\frac{\partial u}{\partial \xi} + \frac{3}{4}\frac{d\overline{U}(\xi)}{d\xi}$$

was not advisable because the values assumed in the upper profile parts on the right side are given as differences of two (approximately equal) large numbers and therefore scatter widely; by this the convergence relations may be concealed. Thus, if one is forced to reduce the step magnitude k still further, one will do so in the manner described above with the aid of the relation (22). It was found that one arrived in this manner, even for the extreme example of the circular cylinder, at a tolerable work expenditure even for the steps immediately ahead of the separation point.

The separation point $\xi = \xi_a$ (and therewith $s = s_a$) is found by graphic interpolation, or extrapolation, of the values $\left[\frac{\partial u}{\partial \eta}\right]_{\eta=0}$ contained in the tables.

The example of the Blasius flow at the flat plate shows very clearly the high degree of accuracy attained with this method. Here the profile obtained by continuation could be compared with the exact profile. After calculation of six steps, the calculated values deviated so little from the exact ones that they could hardly be distinguished within the scope of drawing accuracy. The differences amount to less than 1/2 percent referred to $\overline{U}$.

In order to enable following the mode of calculation in detail, we add the complete calculation of the first step in the continuation of a Blasius profile at the flat plate.

IV. NUMERICAL EXAMPLES AND RESULTS

1. Continuation of a Blasius Profile at the Flat Plate.

The value $s = 0$ is to correspond to the leading edge of the plate. For the boundary-layer equation (3) which because of $p'(s) = 0$ is simplified to

$$v_s \frac{\partial v_s}{\partial s} + v_\eta \frac{\partial v_s}{\partial \eta} = \frac{\partial^2 v_s}{\partial \eta^2}$$

together with the continuity equation

$$\frac{\partial v_s}{\partial s} + \frac{\partial v}{\partial \eta} = 0$$

then exists according to Prandtl-Blasius, as is well known, a solution of the form

$$v_s = \frac{1}{2} U\varphi'(\xi) \qquad \text{with} \qquad \zeta = \frac{1}{2}\sqrt{U}\,\frac{\eta}{\sqrt{s}}$$

for which applies

$$v_s \longrightarrow 0 \qquad \text{for} \qquad \eta \longrightarrow 0$$

$$v_s \longrightarrow U \qquad \text{for} \qquad s \longrightarrow 0 \qquad \text{and all} \quad \eta$$

and

$$v_s \longrightarrow U \qquad \text{for} \qquad \eta \longrightarrow \infty \qquad \text{and all} \quad s \gtreqless 0$$

The function $\varphi = \varphi(\zeta)$ satisfies the ordinary differential equation of the third order

$$\varphi\,\varphi'' = -\,\varphi''' .$$

and the boundary conditions

$$\varphi(0) = 0 \qquad \varphi'(0) = 0 \qquad \lim_{\zeta \to \infty} \varphi'(\zeta) = 2.$$

The values of $\varphi'(\zeta)$ are to be taken from the following table:

ζ	$\frac{1}{2}\varphi'(\zeta)$	ζ	$\frac{1}{2}\varphi'(\zeta)$	ζ	$\frac{1}{2}\varphi'(\zeta)$
0	0				
0.1	0.0664	1.1	0.6813	2.1	0.9670
0.2	0.1328	1.2	0.7290	2.2	0.9759
0.3	0.1989	1.3	0.7725	2.3	0.9827
0.4	0.2647	1.4	0.8115	2.4	0.9878
0.5	0.3298	1.5	0.8460	2.5	0.9915
0.6	0.3938	1.6	0.8761	2.6	0.9942
0.7	0.4563	1.7	0.9018	2.7	0.9962
0.8	0.5168	1.8	0.9233	2.8	0.9975
0.9	0.5748	1.9	0.9411	2.9	0.9984
1.0	0.6298	2.0	0.9555	3.0	0.9990

We choose $U = 1$ so that we may put

$$\xi = s$$

and start our continuation procedure at $s = 1$. As step magnitude in η direction we take $l = 0.6$ so that k becomes equal to 0.18. The initial profile then may be taken directly from the above table, whereas the profile one step farther back, thus the profile at $s = 0.82$, is to be obtained from this table by graphic interpolation. The values are contained in the following table:

η	$u(0.82,\eta)$
0	0
0.6	0.225
1.2	0.430
1.8	0.626
2.4	0.782
3.0	0.894
3.6	0.955
4.2	0.982
4.8	0.995
5.4	1

η	$u(1,\eta)$
0	0
0.6	0.1989
1.2	0.3938
1.8	0.5748
2.4	0.7290
3.0	0.8460
3.6	0.9233
4.2	0.9670
4.8	0.9878
5.4	0.9962
6.0	0.9990
6.6	1

Six steps (that is, up to $s = 2.08$) were calculated by the method described. The calculation of the first step is contained completely in the table added at the end of the report. The results are represented in figure 2.

2. Circular Cylinder According to Hiemenz.

Hiemenz[9] measured the pressure distribution on a circular cylinder of diameter $2r = 9.75$ centimeters immersed in water and approached by the flow at a velocity of 19.2 centimeters per second.

In order to make the quantities appearing in the basic equations dimensionless, one introduces the reference length $l = 1$ centimeter and the reference velocity $V_o = 7.151$ centimeters per second which corresponds for $\nu = 0.01$ centimeter^2 per second to a Reynolds number

$$R = \frac{lV_o}{\nu} = 715.1$$

[9]K. Hiemenz: Die Grenzschicht an einem in den gleichförmigen Flüssigkeitsstrom eingetauchten geraden Kreiszylinder (The boundary layer on a rectilinear circular cylinder immersed in the uniform fluid flow). Dissertation Göttingen, 1911, published in Dingler's polytechn. J. Vol. 326, 1911, pp. 321-342.

then the velocity distribution measured for $0 \leqq s \leqq 7$, that is up to the separation point, observed shortly before $s = 7$ (corresponding to an angle α of 80° to 82° from the forward stagnation point) may be represented satisfactorily by the polynomial

$$U(s) = s - 0.006289\, s^3 - 0.000046\, s^5$$

On the basis of the previous indication, the solution of Blasius-Hiemenz could be used up to the value $s = 4.5$ $(\alpha \sim 55^{\circ})$ so that our calculation starts at $s = 4.5$ (as does Görtler's[10]). The value $l = 0.4$, and thus $k = 0.08$ were selected as step magnitudes for the first steps. The representation of

$$\xi = \int_{4.5}^{s} \frac{1}{U(t)}\, dt \text{ and } U = U(s)$$

against s may be seen from figure 3.

The initial profiles at $\xi = -0.08$ and $\xi = 0$, taken from Howarth's tables, are compiled, together with the values of $\left[\frac{\partial u}{\partial s}\right]_{s=4.5}$ resulting from the same tables, in the following table:

η	$u(-0,08,\eta)$	$u(0,\eta)$	$\left[\frac{\partial v_s}{\partial s}\right]_{s=4.5}$
0	0	0	0
0.4	1.282	1.289	0.008
0.8	2.229	2.2268	0.104
1.2	2.871	2.948	0.249
1.6	3.269	3.384	0.367
2.0	3.488	3.628	0.448
2.4	3.596	3.749	0.497
2.8	3.649	3.813	0.529
3.2	3.667	3.834	0.538
3.6	3.672	3.839	0.540
∞	3.674	3.842	

When the latter values are used, the calculation of the first step requires only one worksheet of the type described before. With the step magnitudes indicated, first four steps (up to $\xi = 0.32$) were calculated.

[10]See footnote 3.

The profiles obtained are represented together with the initial profiles in figure 4 (partly displaced with respect to each other).

With the initial relations (22) as a basis, five further steps (up to $\xi = 0.52$) were calculated for the same $l = 0.4$ and the required $k = 0.04$. Likewise with the use of equation (22), one step ($\xi = 0.54$) with $l = \sqrt{0.08} = 0.283$ and $k = 0.02$ and finally two more steps with $l = 0.2$, $k = 0.01$ (up to $\xi = 0.56$) were calculated. The profiles are also represented in figure 5.

By plotting of the values $\frac{\partial u(\xi_\rho,0)}{\partial \eta}$ the separation point was found to be $\xi_{sep} = 0.5697$, that is $s_{sep} = 6.87$ (compare figure 6). Thus all together twelve steps were to be calculated. Figure 7 shows the curves $u = u(\xi, \text{const})$. Their steep decline in the neighborhood of the separation point is remarkable.

Figure 8 shows a comparison of a few of the profiles obtained by us (-S) with those of Blasius-Hiemenz (— --B-H), Pohlhausen (— - —P), and Görtler (— —G) which were obtained for the same pressure distribution[11]. The comparison shows, first of all, that the Blasius-Hiemenz solution becomes insufficient in the neighborhood of the separation point; the reason obviously lies in the fact that the series developments used converge for large s only slowly, if at all, and that, therefore, with merely the first three terms the actual course is not satisfactorily represented there.

Our values agree best and most systematically with those obtained by Görtler. The differences are increasingly noticeable toward the separation point. The deviations from the values obtained by Pohlhausen, considered as a whole, remain for this example within tolerable limits although a systematic variation of the differences cannot be determined. It is remarkable that the differences assume higher values precisely in the proximity of the velocity maximum ($\xi \sim 0.36$, $s \sim 6$, $\alpha \sim 71^\circ$) (compare the curve for $\xi \doteq 0.32$ represented in figure 8) while again subsiding to some extent toward the separation point.

The separation point was found according to Görtler in good agreement with our value $s_{sep} = 6.8$, according to Hiemenz at $s_{sep} = 6.98$, and according to Pohlhausen at $s_{sep} = 6.94$. An approximately correct position of the separation point is, therefore, by itself not yet decisive for the usefulness of a method.

[11]Compare K. Hiemenz, paper quoted in footnote 9, H. Görtler, paper quoted in footnote 3, and K. Pohlhausen, "Zur näherungsweisen Integration der Differentialgleichung der laminaren Grenzschicht" (On the approximate integration of the differential equation of the laminar boundary layer), Z.A.M.M. Bd. 1, 1921, pp. 252-268.

3. Elliptic Cylinder of the Aspect Ratio 1:4.

As a further example, we calculated the boundary layer for an elliptic cylinder of the aspect ratio 1:4, taking as a basis the pressure distribution resulting from the potential theory.

$$l = \frac{l_o}{10} \text{ and } V_o = 4.3\ U_o$$

were chosen as reference quantities for the introduction of dimensionless quantities, with l_o being half the circumference of the ellipse and U_o the free stream velocity. The (dimensionless) velocity at the edge of the boundary layer could be taken directly from a table by Schlichting and Ulrich.[12] It is represented in figure 9 together with the function

$$\xi = \xi(s) = \int_{0.2}^{s} \frac{dt}{U(t)}$$

In the interval $0 \leqq s \leqq 0.2$ it was possible to represent $U = U(s)$ satisfactorily by the polynomial

$$U(s) = s - 5.116\ s^3$$

The initial profile, however, was chosen at $s = 0.163$ ($\xi = -0.25$) for the reasons mentioned before. For the first six steps $l = 0.5$ and $k = 0.125$ were taken as step magnitudes. The two initial profiles are represented in the following table, together with the values $\left[\frac{\partial v_s}{\partial s}\right]_{s = 0.163}$.

η	$u(-0.375,\eta)$	$u(-0.25,\eta)$	$\left[\frac{\partial v_s}{\partial s}\right]_{s = 0.163}$
0	0	0	0
0.5	0.0573	0.0589	0.0949
1.0	0.0951	0.0990	0.2672
1.5	0.1166	0.1226	0.4235
2.0	0.1268	0.1340	0.5197
2.5	0.1310	0.1389	0.5703
3.0	0.1323	0.1403	0.5858
	0.1327	0.1408	

[12] H. Schlichting und A. Ulrich, "Zur Berechnung des Umschlages laminar-turbulent" (On the calculation of the transition from laminar to turbulent) Bericht S 10 der Lilienthal-Gesellschaft (1940), pp. 75-135.

From $\xi = 0.5$ onward the steps could, first, be increased. The following further steps were calculated: Seven steps with $l = \sqrt{0.5} = 0.7071$ and $k = 0.25$ (up to $\xi = 2.25$), three steps with $l = 1$, $k = 0.5$ (up to $\xi = 3.75$), four steps with $l = \sqrt{2} = 1.414$ and $k = 1$ (up to $\xi = 7.75$), and nine steps with $l = 2$ and $k = 2$ (up to $\xi = 25.75$).

With the aid of the starting equation (22) another step reduction was made. The further steps were: Three steps with $l = 2$ and $k = 1$ (up to $\xi = 28.75$) and finally one step with $l = \sqrt{2} = 1.414$ and $k = 0.5$ (up to $\xi = 29.25$). A complete calculation was thus made of 33 steps altogether.

It became clear that selection of larger steps is not advisable, particularly at the point where the curve $U = U(s)$ turns from its steep ascent to the flatter course (compare figure 12).

On the "high plateau" of velocity distribution itself one could have chosen steps somewhat larger but they would have had to be reduced again when approaching the separation point. A large number of the profiles we calculated can be seen in figure 10. The separation point was determined from the variation of $\left[\frac{\partial u}{\partial \eta}\right]_{\eta=0}$ as $s_{sep} = 8.475$ (compare figure 11).

Since Schlichting and Ulrich completely calculated[13] the same example once according to the ordinary Pohlhausen method (P_4-method), and then according to a Pohlhausen method modified by taking a polynomial of the sixth degree as a basis (P_6-method), the comparison could be made for a number of profiles. The results are compiled in figures 13 and 14.

As far as the pressure minimum the deviations between our curves and the P_4- and P_6-curves are not too large. However, larger deviations appear in the proximity of the separation point. There the profiles of the original Pohlhausen method agree with ours better than the profiles of the P_6-method, especially for small η values. The resulting separation point was, according to the P_4-method, at $s_{sep} = 8.38$, according to the P_6-method, at $s_{sep} = 8.26$; thus these values (especially that of the P_4-method) do not deviate too widely from our value.

---

[13]Quoted in footnote 12.

V. REMARKS REGARDING THE CONVERGENCE OF THE ITERATION PROCESS

Regarding the conditions of convergence of the iteration process described in section III, we can prove the following theorem which will probably be sufficient for the requirements of practical calculation. If there applies for the profile at the point $\xi = \xi_\rho$ for all $\eta \leqq \eta\sigma_o$

$$0 \leqq [u]_{\xi_\rho,\eta} < \overline{U}(\xi_\rho)$$

and

$$\frac{\eta\left|\frac{\partial u}{\partial \eta}\right|_{\xi_\rho,\eta}}{\overline{U}(\xi_\rho)} < 1 + \frac{[u]_{\xi_\rho,\eta}}{\overline{U}(\xi_\rho)}$$

the sequence of the velocity values obtained by the iteration process

$$[u_n]_{\rho+1,\sigma} \quad (\sigma \leqq \sigma_o)$$

converges with increasing n.

Thus one is always able to predict, when calculating a new step, whether the iteration process will converge. The presuppositions of the theorem are satisfied with certainty when for all $\eta \leqq \eta\sigma_o$

$$0 \leqq [u]_{\xi_\rho,\eta} < \overline{U}(\xi_\rho) \text{ and } \left[\frac{\partial^2 u}{\partial \eta^2}\right]_{\xi_\rho,\eta} \leqq 0$$

apply as is the case for instance for the profiles before the pressure minimum; for then

$$\eta\left[\frac{\partial u}{\partial \eta}\right]_{\xi_\rho,\eta} \leqq \eta\left[\frac{\partial u}{\partial \eta}\right]_{\xi_\rho,\eta^*} = [u]_{\xi_\rho,\eta} < \overline{U}(\xi_\rho)$$

is valid if η^* is selected so that

$$[u]_{\xi_\rho,\eta} = \eta\left[\frac{\partial u}{\partial \eta}\right]_{\xi_\rho,\eta^*} \qquad (\eta \leqq \eta\sigma_o)$$

The presuppositions are satisfied also for the S-shaped profiles beyond the pressure minimum when $\frac{\partial u}{\partial \eta}$ does not become too large. For the examples we calculated, boundary-layer flow for circular and elliptic cylinder, the presuppositions are satisfied, up to the separation point. Proof of the theorem: If one takes into consideration that according to the procedure of section III one has to put

$$\left[u^*_{n+1}\right]_{\rho+1,\sigma} = \frac{u^*_{\rho,\sigma+1} + u^*_{\rho,\sigma-1}}{2} +$$

$$\frac{k}{\overline{U}(\xi_\rho)}\left[\frac{\partial u}{\partial \eta}\right]_{\xi_\rho,\eta_\sigma} \quad l \left\{\sum_{\tau=1}^{\sigma-1} \frac{\left[u_u\right]_{\rho+1,\tau} - u_{\rho-1,\tau}}{2k} + \right.$$

$$\left. \frac{1}{2}\,\frac{\left[u_u\right]_{\rho+1,\sigma} - u_{\rho-1,\sigma}}{2k}\right\} -$$

$$\frac{k}{\overline{U}(\xi_\rho)}\, u^*_{\rho,\sigma}\, \frac{\left[u_u\right]_{\rho+1,\sigma} - u_{\rho-1,\sigma}}{2k}$$

there follows with

$$\left[d_n\right]_{\rho+1,\sigma} = \underset{\tau=1,2,\ldots,\sigma}{\mathrm{Max}} \left\{\left|\left[u_n\right]_{\rho+1,\tau} - \left[u_{n-1}\right]_{\rho+1,\tau}\right|\right\} \qquad (\sigma \leqq \sigma_o)$$

with the presuppositions taken into consideration, obviously

$$\left|\left[u_{u+1}\right]_{\rho+1,1} - \left[u_u\right]_{\rho+1,1}\right| \leqq \frac{1}{2\overline{U}(\xi_\rho)}\, \eta_1 \left|\frac{\partial u}{\partial \eta}\right|_{\xi_\rho,\eta_1} \left[d_u\right]_{\rho+1,\sigma} +$$

$$\frac{1}{2\overline{U}(\xi_\rho)}\left(\overline{U}(\xi_\rho) - u_{\rho,1}\right)\left[d_n\right]_{\rho+1,\sigma}$$

$$\leqq \alpha \left[d_u\right]_{\rho+1,\sigma}$$

with $0 < \alpha < 1$ and α beind independent of n. Furthermore, one can see for oneself that α $(0 < \alpha < 1$, independent of $n)$ can be chosen so that simultaneously the estimations

$$\left|\left[u_{u+1}\right]_{\rho+1,\sigma} - \left[u_u\right]_{\rho+1,2}\right| \leqq \alpha \left[d_u\right]_{\rho+1,\sigma}$$

$$\vdots$$

$$\left|\left[u_{u+1}\right]_{\rho+1,\sigma} - \left[u_u\right]_{\rho+1,\sigma}\right| \leqq \alpha \left[d_u\right]_{\rho+1,\sigma}$$

exist so that

$$\left[d_{u+1}\right]_{\rho+1,\sigma} \leqq \alpha \left[d_n\right]_{\rho+1,\sigma}$$

must be true as well.

Hence there exists the limit

$$\begin{aligned} u_{\rho+1,\sigma} &= \lim_{\eta \longrightarrow \infty} \left[u_n\right]_{\rho+1,\sigma} \\ &= \left[u_1\right]_{\rho+1,\sigma} + \left(\left[u_2\right]_{\rho+1,\sigma} - \left[u_1\right]_{\rho+1,\sigma}\right) + \ldots + \\ &\quad \left(\left[u_u\right]_{\rho+1,\sigma} - \left[u_{n-1}\right]_{\rho+1,\sigma}\right) + \ldots \quad (\sigma \leqq \sigma_0) \end{aligned}$$

since the series at right may be majorized by a convergent geometrical series.

One recognizes further that - if equations (18) or (19) are used instead of equation (15) - if convergence of the iteration process can be proved under the assumptions that for $\xi = \xi_\rho$ and all $\eta \leqq \eta_\sigma$

$$0 \leqq [u]_{\xi_\rho,\eta} < \overline{U}(\xi_\rho)$$

and

$$\eta \left|\frac{\partial u}{\partial \eta}\right|_{\xi_\rho, \eta} < [u]_{\xi_\rho, \eta}$$

since one then finds the estimations

$$\left|\left[u_{u+1}\right]_{\rho+1,1} - \left[u_u\right]_{\rho+1,1}\right| < \left(\frac{[u]_{\xi_\rho,\eta_1}}{\overline{U}(\xi_\rho)} + \frac{\overline{U}(\xi_\rho) - [u]_{\xi_\rho,\eta_1}}{\overline{U}(\xi_\rho)}\right)\left[d_u\right]_{\rho+1,\sigma}$$

$$\vdots$$

$$\left|\left[u_{u+1}\right]_{\rho+1,\sigma} - \left[u_u\right]_{\rho+1,\sigma}\right| < \left(\frac{[u]_{\xi_\rho,\eta_\sigma}}{\overline{U}(\xi_\rho)} + \frac{\overline{U}(\xi_\rho) - [u]_{\xi_\rho,\eta_\sigma}}{\overline{U}(\xi_\rho)}\right)\left[d_u\right]_{\rho+1,\sigma}$$

thus

$$\left[d_{u+1}\right]_{\rho+1,\sigma} \leqq \alpha \left[d_u\right]_{\rho+1,\sigma}$$

again with $0 < \alpha < 1$ and α independent of n. These presuppositions are satisfied for instance for the profiles before the pressure minimum. However, in the proximity of the wall, if the profiles there show an approximately rectilinear course, the convergence will take place only very slowly.

Beyond the pressure minimum one can, therefore, not arrive at a general statement on the convergence. As mentioned before, our calculations in the proximity of the separation point showed that the case of divergence may actually occur. Therewith the procedure we selected, using the relation (19) merely for the correction calculation, proves to be perfectly reasonable also from the general point of view now considered.

Correspondingly, one recognizes that the iteration process performed with the aid of relation (22) certainly is convergent at the point $\xi = \xi_\rho$ for $\sigma \leqq \sigma_0$ if there for all $\eta \leqq \eta\sigma_0$

$$0 \leqq [u]_{\xi_\rho,\bar{\eta}} < \overline{U}(\xi_\rho)$$

and

$$\frac{\eta \left|\frac{\partial u}{\partial \eta}\right|_{\xi_\rho,\eta}}{\overline{U}(\xi_\rho)} < \begin{cases} \frac{1}{2} + \frac{[u]_{\xi_\rho,\eta}}{\overline{U}(\xi_\rho)} \text{ for } \frac{[u]_{\xi_\rho,\eta}}{\overline{U}(\xi_\rho)} \leqq \frac{1}{2} \\ \frac{1}{2} + \left(1 - \frac{[u]_{\xi_\rho,\eta}}{\overline{U}(\xi_\rho)}\right) \text{ for } \frac{[u]_{\xi_\rho,\eta}}{\overline{U}(\xi_\rho)} > \frac{1}{2} \end{cases}$$

If one takes generally the initial relation

$$\frac{1}{m}\frac{\partial u^*}{\partial \xi} - \frac{\partial^2 u^*}{\partial \eta^2} = \frac{1}{\overline{U}(\xi)}\frac{\partial u}{\partial \eta}\int_0^\eta \frac{\partial u}{\partial \xi}\,d\eta - \left(\frac{u^*}{\overline{U}(\xi)} + \left(1 - \frac{1}{m}\right)\right)\frac{\partial u}{\partial \xi} +$$

$$\left(1 - \frac{1}{m}\right)\frac{d\overline{U}(\xi)}{d\xi} \qquad (m \geqq 1)$$

convergence at the point $\xi = \xi_\rho$ for $\sigma \leqq \sigma_o$ would be assured under the following sufficient conditions: For all $\eta \leqq \eta\sigma_o$ there shall be valid

$$0 \leqq [u]_{\xi_\rho,\eta} < \overline{U}(\xi_\rho)$$

and

$$\frac{\eta \left|\frac{\partial u}{\partial \eta}\right|_{\xi_\rho,\eta}}{\overline{U}(\xi_\rho)} < \begin{cases} \frac{1}{m} + \frac{[u]_{\xi_\rho,\eta}}{\overline{U}(\xi_\rho)} \text{ for } \frac{[u]_{\xi_\rho,\eta}}{\overline{U}(\xi_\rho)} \leqq \frac{1}{m} \\ \frac{1}{m} + \left(\frac{2}{m} - \frac{[u]_{\xi_\rho,\eta}}{\overline{U}(\xi_\rho)}\right) \text{ for } \frac{[u]_{\xi_\rho,\eta}}{\overline{U}(\xi_\rho)} > \frac{1}{m} \end{cases}$$

Thus, if one wants on the right side a positive limit also for

$$\left[u\right]_{\xi_\rho,\eta} \xrightarrow{(\eta\rightarrow\infty)} \bar{U}(\xi_\rho)$$

m must be not greater than 3.

Translated by Mary L. Mahler
National Advisory Committee
for Aeronautics

TABLE I.

η_σ	$\alpha_\sigma = \left[\frac{\partial u}{\partial \xi}\right]_{0,\sigma}$	$\beta_\sigma = \int_0^{\eta_\sigma} \left[\frac{\partial u}{\partial \xi}\right]_{0,\sigma} d\eta$	$\left[\frac{\partial u}{\partial \eta}\right]_{0,\sigma}$	$\gamma_\sigma = \frac{k}{\overline{U}(0)} \left[\frac{\partial u}{\partial \eta}\right]_{0,\sigma}$	$A_\sigma = \beta_\sigma \gamma_\sigma$	$\epsilon_\sigma = \frac{k}{\overline{U}(0)} \left[u^*\right]_{0,\sigma}$	$B_\sigma = -\alpha_\sigma \epsilon_\sigma$	$A_\sigma + B_\sigma$	$C_\sigma = \frac{u_{0,\sigma+1} + u_{0,\sigma-1}}{2}$	$\left[u^*_1\right]_{1,\sigma} = A_\sigma + B_\sigma + C_\sigma$	$\left[u_1\right]_{1,\sigma} = \left[u^*_1\right]_{1,\sigma} + \overline{U}(\xi_1)$
0	0	0	*		0		0	0		$-\overline{U}(\xi_1)$	0
l	*	*	*	*	*	*	*	*	*	*	*
$2l$	*	*	*	*	*	*	*	*	*	*	*
⋮	⋮	⋮	⋮	⋮	⋮	⋮	⋮	⋮	⋮	⋮	⋮

TABLE II.

η_σ	$\alpha_\sigma = \left[\frac{\partial u_1}{\partial \xi}\right]_{0,\sigma}$	$\beta_\sigma = \int_0^{\eta_\sigma} \left[\frac{\partial u_1}{\partial \xi}\right]_{0,\sigma} d\eta$	$A_\sigma = \beta_\sigma \gamma_\sigma$	$B_\sigma = -\alpha_\sigma \epsilon_\sigma$	$A_\sigma + B_\sigma$	$\left[u_2^*\right]_{1,\sigma} = A_\sigma + B_\sigma + C_\sigma$	$\left[u_2\right]_{1,\sigma} = \left[u_2^*\right]_{1,\sigma} + \overline{U}(\xi_1)$	D_σ	$\left[\overline{u}_2^*\right]_{1,\sigma} = D_\sigma + 2(A_\sigma + B_\sigma)$	$\left[\overline{u}_2\right]_{1,\sigma} = \left[\overline{u}_2^*\right]_{1,\sigma} + \overline{U}(\xi_1)$
0	0	0	0	0	0	$-\overline{U}(\xi_1)$	0		$-\overline{U}(\xi_1)$	0
l	*	*	*	*	*	*	*	*	*	*
$2l$	*	*	*	*	*	*	*	*	*	*
⋮	⋮	⋮	⋮	⋮	⋮	⋮	⋮	⋮	⋮	⋮

TABLE III.

η_σ	$\alpha_\sigma = \left[\frac{\partial u_2}{\partial \xi}\right]_{0,\sigma}$	$\beta_\sigma = \int_0^{\eta_\sigma} \left[\frac{\partial u_2}{\partial \xi}\right]_{0,\sigma} d\eta$	$A_\sigma = \beta_\sigma \gamma_\sigma$	$B_\sigma = -\alpha_\sigma \epsilon_\sigma$	$A_\sigma + B_\sigma$	$\left[\overline{u}_3^*\right]_{1,\sigma} = D_\sigma + 2(A_\sigma + B_\sigma)$	$\left[\overline{u}_3\right]_{1,\sigma} = \left[\overline{u}_3^*\right]_{1,\sigma} + \overline{U}(\xi_1)$
0	0	0	0	0	0	$-\overline{U}(\xi_1)$	0
l	*	*	*	*	*	*	*
$2l$	*	*	*	*	*	*	*
⋮	⋮	⋮	⋮	⋮	⋮	⋮	⋮

THE FIRST STEP IN THE CONTINUATION OF

THE BLASIUS PROFILE

I

η_σ	$\alpha_\sigma = \left[\frac{\partial u}{\partial \xi}\right]_{0,\sigma}$	$\beta_\sigma = \int_0^{\eta_\sigma}\left[\frac{\partial u}{\partial \xi}\right]_{0,\sigma} d\eta$	$\left[\frac{\partial u}{\partial \eta}\right]_{0,\sigma}$	$\gamma_\sigma = 0.18\left[\frac{\partial u}{\partial \eta}\right]_{0,\sigma}$	$A_\sigma = \beta_\sigma\gamma_\sigma$	$\epsilon_\sigma = 0.18\left[u^*\right]_{0,\sigma}$	$B_\sigma = -\alpha_\sigma\epsilon_\sigma$	$A_\sigma + B_\sigma$	$C_\sigma = \frac{u^*_{0,\sigma+1} + u^*_{0,\sigma-1}}{2}$	$\left[u_1^*\right]_{1,\sigma} = A_\sigma + B_\sigma + C_\sigma$	$\left[u_1\right]_{1,\sigma} = \left[u_1^*\right]_{1,\sigma} + 1$
0	0	0	0.3282		0		0	0		-1.0000	0
0.6	-0.1450 -0.3461	-0.0435 -0.1038	0.3282	0.05908	-0.0026	-0.14420	-0.0209	-0.0235	-0.8031	-0.8266	0.1734
1.2	-0.2011 -0.4855	-0.1473 -0.1457	0.3132	0.05638	-0.0083	-0.10912	-0.0219	-0.0302	-0.6132	-0.6434	0.3566
1.8	-0.2844 -0.5788	-0.2930 -0.1736	0.2793	0.05027	-0.0147	-0.07654	-0.0218	-0.0365	-0.4386	-0.4751	0.5249
2.4	-0.2944 -0.5611	-0.4666 -0.1683	0.2260	0.04068	-0.0190	-0.04878	-0.0144	-0.0334	-0.2896	-0.3230	0.6770
3.0	-0.2667 -0.4428	-0.6349 -0.1328	0.1619	0.02914	-0.0185	-0.02772	-0.0074	-0.0259	-0.1739	-0.1998	0.8002
3.6	-0.1761 -0.2594	-0.7677 -0.0778	0.1008	0.01814	-0.0139	-0.01381	-0.0024	-0.0163	-0.0935	-0.1098	0.8902
4.2	-0.0833 -0.1233	-0.8455 -0.0370	0.0537	0.00967	-0.0082	-0.00594	-0.0005	-0.0087	-0.0445	-0.0532	0.9468
4.8	-0.0400 -0.0611	-0.8825 -0.0183	0.0243	0.00437	-0.0039	-0.00220	-0.0001	-0.0040	-0.0184	-0.0224	0.9776
5.4	-0.0211 -0.0267	-0.9008 -0.0080	0.0093	0.00167	-0.0015	-0.00068	0	-0.0015	-0.0066	-0.0081	0.9919
6.0	-0.0056 -0.0056	-0.9088 -0.0017	0	0	0	0	0	0	-0.0019	-0.0019	0.9981
6.6	0	-0.9105	0	0	0	0	0	0	-0.0005	-0.0005	0.9995
7.2	0	-0.9105	0	0	0	0	0	0	0	0	1

II

η_σ	$\alpha_\sigma = \left[\frac{\partial u_1}{\partial \xi}\right]_{0,\sigma}$	$\beta_\sigma = \int_0^{\eta_\sigma} \left[\frac{\partial u_1}{\partial \xi}\right]_{0,\sigma} d\eta$	$A_\sigma = \beta_\sigma \gamma_\sigma$	$B_\sigma = -\alpha_\sigma \epsilon_\sigma$	$A_\sigma + B_\sigma$	$\left[u_2^*\right]_{1,\sigma} = A_\sigma + B_\sigma + C_\sigma$	$\left[u_2\right]_{1,\sigma} = \left[u_2^*\right]_{1,\sigma} + 1$	D_σ	$\left[\bar{u}_2^*\right]_{1,\sigma} = D_\sigma + 2(A_\sigma + B_\sigma)$	$\left[\bar{u}_2\right]_{1,\sigma} = \left[\bar{u}_2^*\right]_{1,\sigma} + 1$
0	0	0	0	0	0	1.0000	0		-1.0000	0
0.6	-0.1433 -0.3472	-0.0430 -0.1042	-0.0025	-0.0207	-0.0232	-0.8263	0.1737	-0.7795	-0.8259	0.1741
1.2	-0.2039 -0.4847	-0.1472 -0.1454	-0.0083	-0.0222	-0.0305	-0.6437	0.3563	-0.5847	-0.6457	0.3543
1.8	-0.2808 -0.5725	-0.2926 -0.1718	-0.0147	-0.0215	-0.0362	-0.4748	0.5252	-0.4002	-0.4726	0.5274
2.4	-0.2917 -0.5522	-0.4644 -0.1657	-0.0189	-0.0142	-0.0331	-0.3227	0.6773	-0.2532	-0.3194	0.6806
3.0	-0.2605 -0.4405	-0.6301 -0.1322	-0.0184	-0.0072	-0.0256	-0.1995	0.8005	-0.1436	-0.1948	0.8052
3.6	-0.1800 -0.2778	-0.7623 -0.0833	-0.0138	-0.0025	-0.0163	-0.1098	0.8902	-0.0775	-0.1101	0.8899
4.2	-0.0978 -0.1461	-0.8456 -0.0438	-0.0082	-0.0006	-0.0088	-0.0533	0.9467	-0.0410	-0.0586	0.9414
4.8	-0.0483 -0.0708	-0.8894 -0.0212	-0.0039	-0.0001	-0.0040	-0.0224	0.9776	-0.0183	-0.0263	0.9737
5.4	-0.0225 -0.0278	-0.9106 -0.0083	-0.0015	0	-0.0015	-0.0081	0.9919	-0.0073	-0.0103	0.9897
6.0	-0.0053 -0.0067	-0.9189 -0.0020	0	0	0	-0.0019	0.9981	-0.0028	-0.0028	0.9972
6.6	-0.0014	-0.9209	0	0	0	-0.0005	0.9995	0	0	1
7.2	0	-0.9209	0	0	0	0	1	0	0	1

III

η_σ	$\alpha_\sigma = \left[\frac{\partial u_2}{\partial \xi}\right]_{0,\sigma}$	$\beta_\sigma = \int_0^{\eta_\sigma} \left[\frac{\partial u_2}{\partial \xi}\right]_{0,\sigma} d\eta$	$A_\sigma = \beta_\sigma \gamma_\sigma$	$B_\sigma = -\alpha_\sigma \epsilon_\sigma$	$A_\sigma + B_\sigma$	$\left[\bar{u}_3^*\right]_{1,\sigma} = D_\sigma + 2(A_\sigma + B_\sigma)$	$\left[\bar{u}_3\right]_{1,\sigma} = \left[\bar{u}_3\right]_{1,\sigma} + 1$
0	0	0	0	0	0	1.0000	0
0.6	-0.1414 -0.3517	-0.0424 -0.1055	-0.0025	-0.0204	-0.0229	-0.8253	0.1747
1.2	-0.2103 -0.4842	-0.1479 -0.1453	-0.0083	-0.0229	-0.0312	-0.6471	0.3529
1.8	-0.2739 -0.5556	-0.2932 -0.1667	-0.0147	-0.0210	-0.0357	-0.4716	0.5284
2.4	-0.2817 -0.5284	-0.4599 -0.1585	-0.0187	-0.0137	-0.0324	-0.3180	0.6820
3.0	-0.2467 -0.4275	-0.6184 -0.1283	-0.0180	-0.0068	-0.0248	-0.1932	0.8068
3.6	-0.1808 -0.2936	-0.7467 -0.0881	-0.0135	-0.0025	-0.0160	-0.1095	0.8905
4.2	-0.1128 -0.1720	-0.8348 -0.0516	-0.0081	-0.0007	-0.0088	-0.0586	0.9414
4.8	-0.0592 -0.0878	-0.8864 -0.0263	-0.0039	-0.0001	-0.0040	-0.0263	0.9737
5.4	-0.0286 -0.0364	-0.9127 -0.0109	-0.0015	0	-0.0015	-0.0103	0.9897
6.0	-0.0078 -0.0078	-0.9236 -0.0023	0	0	0	-0.0028	0.9972
6.6	0	-0.9259	0	0	0	0	1
7.2	0	-0.9259	0	0	0	0	1

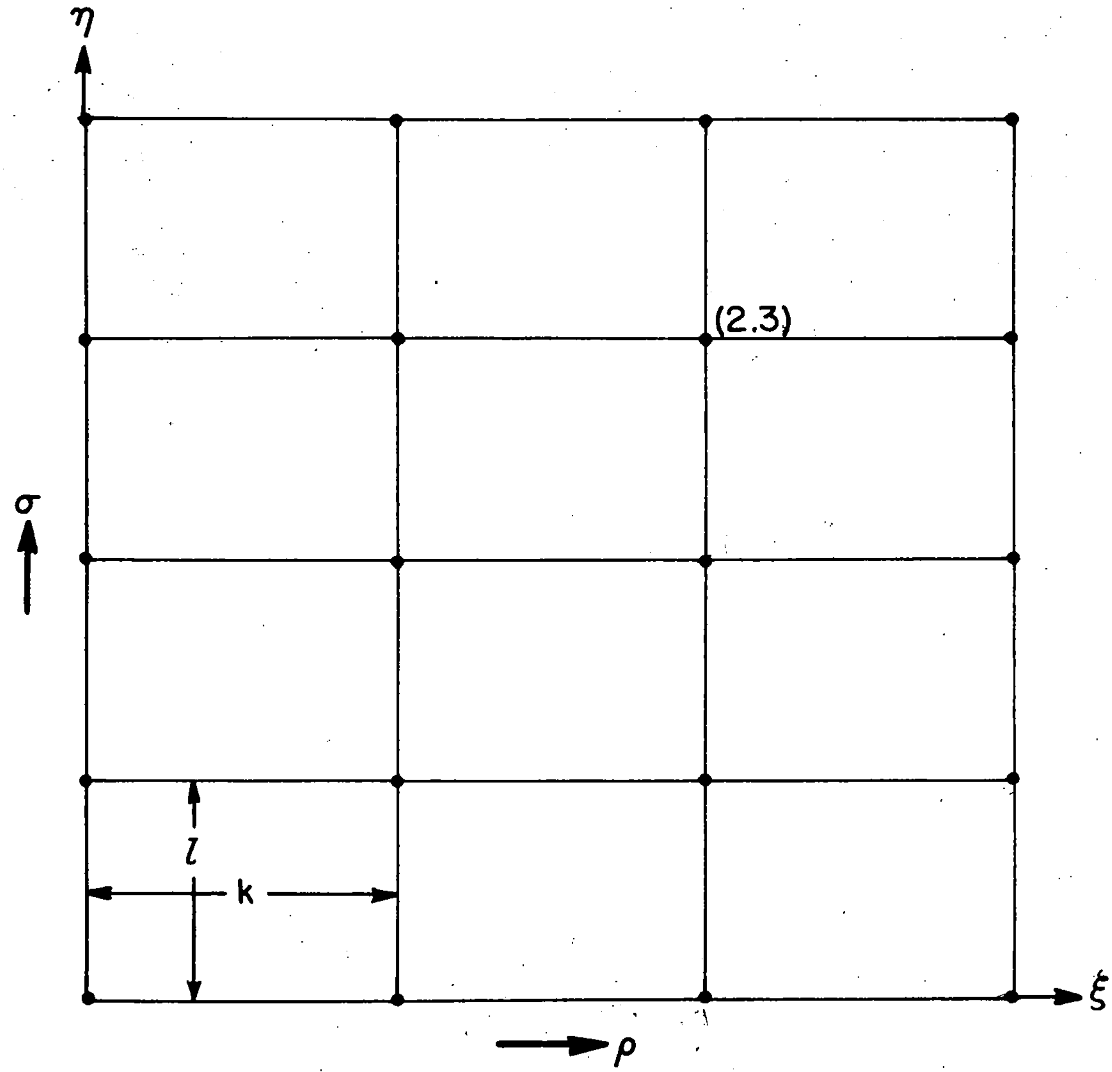

Figure 1.- The net of the lattice points.

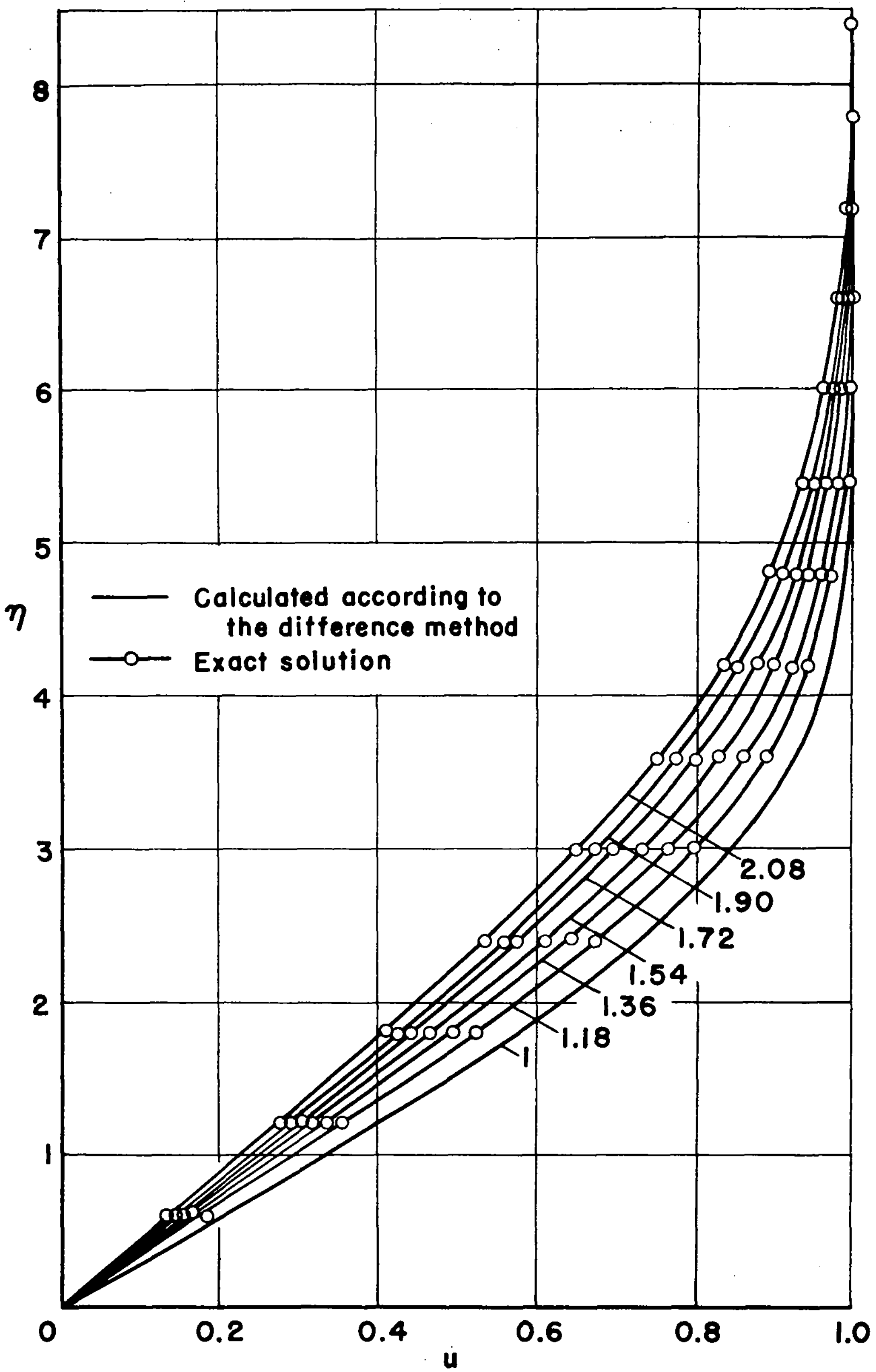

Figure 2.- Continuation of a Blasius profile at the flat plate.

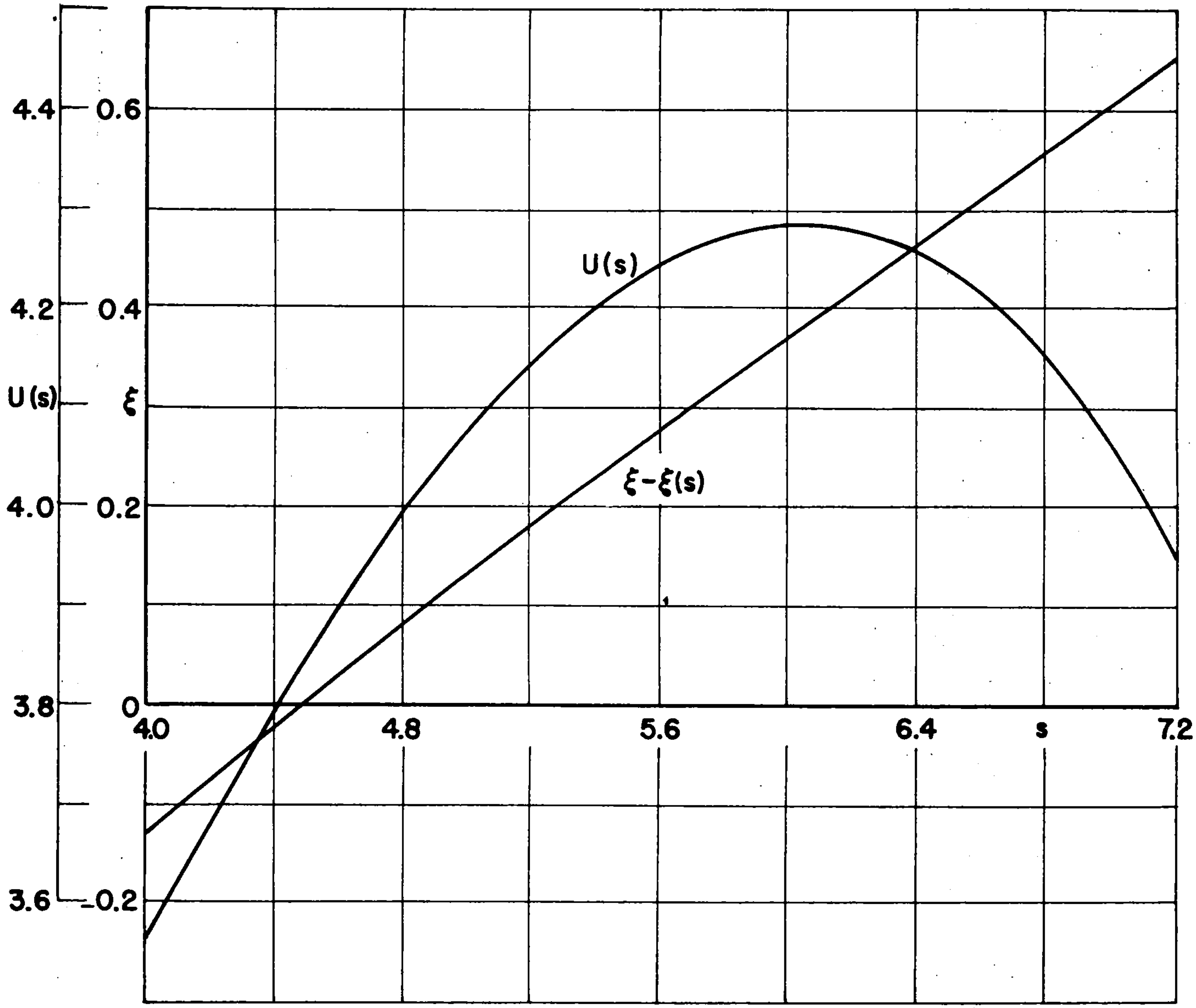

Figure 3.- The functions $\xi = \xi(s)$, $U = U(s)$ for the circular cylinder.

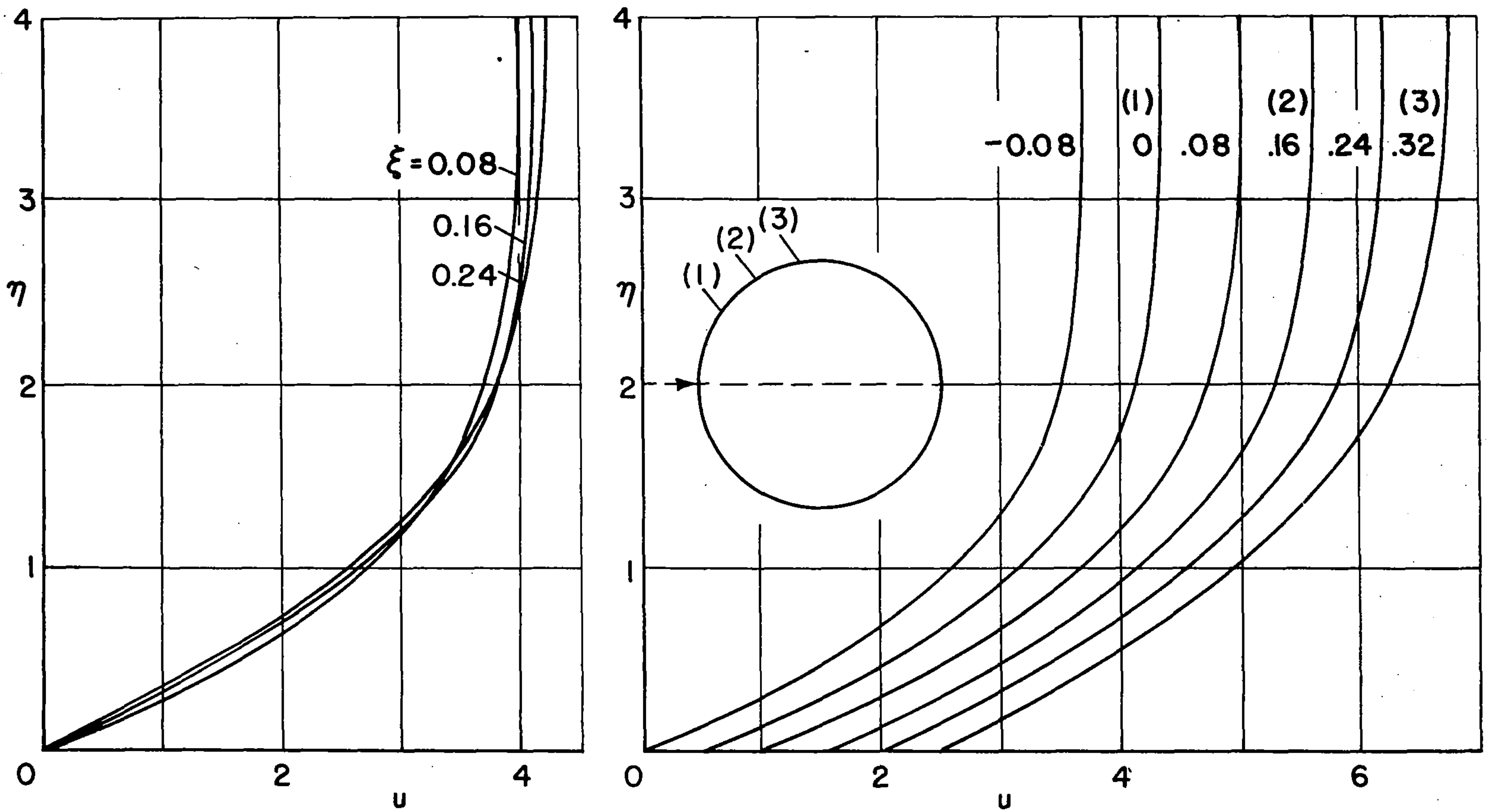

Figure 4.- The four first profiles calculated according to the difference method for the circular cylinder.

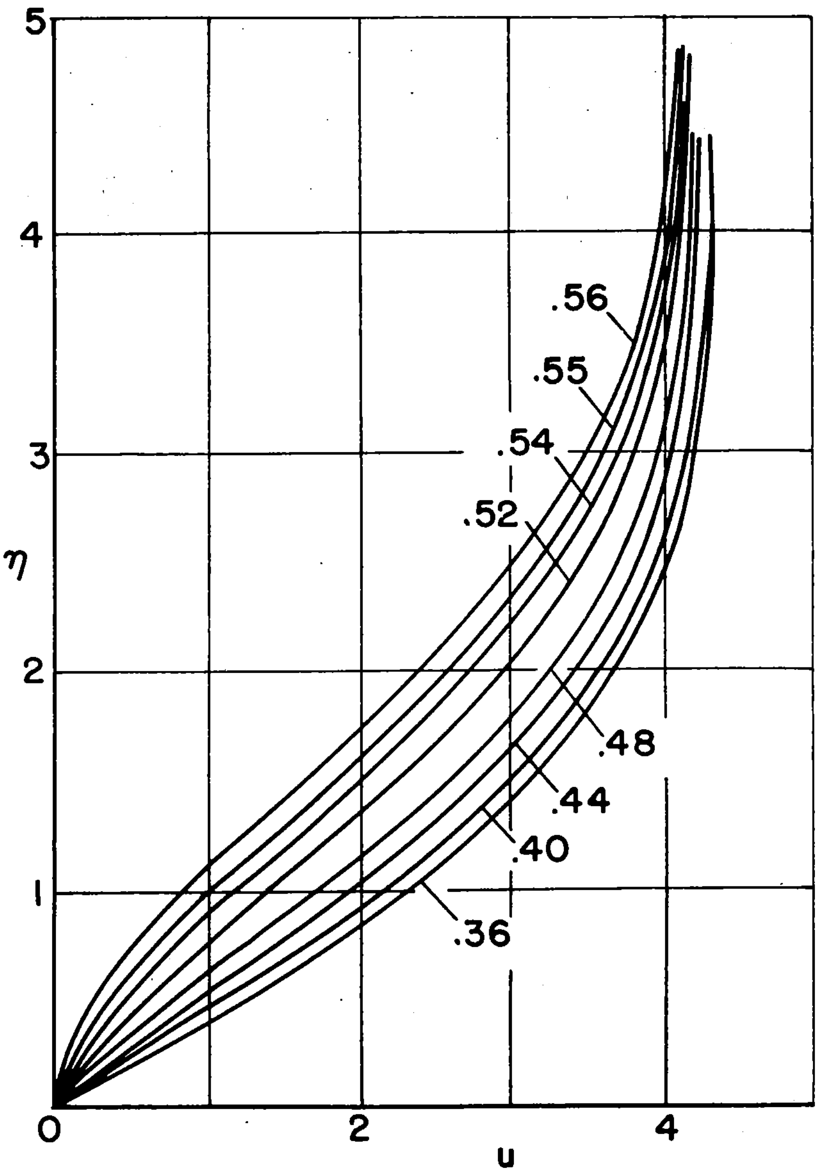

Figure 5.- Further profiles for the circular cylinder.

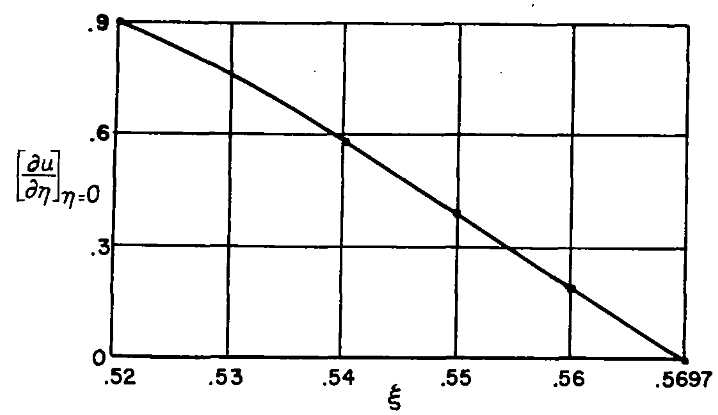

Figure 6.- Determination of the separation point for the circular cylinder

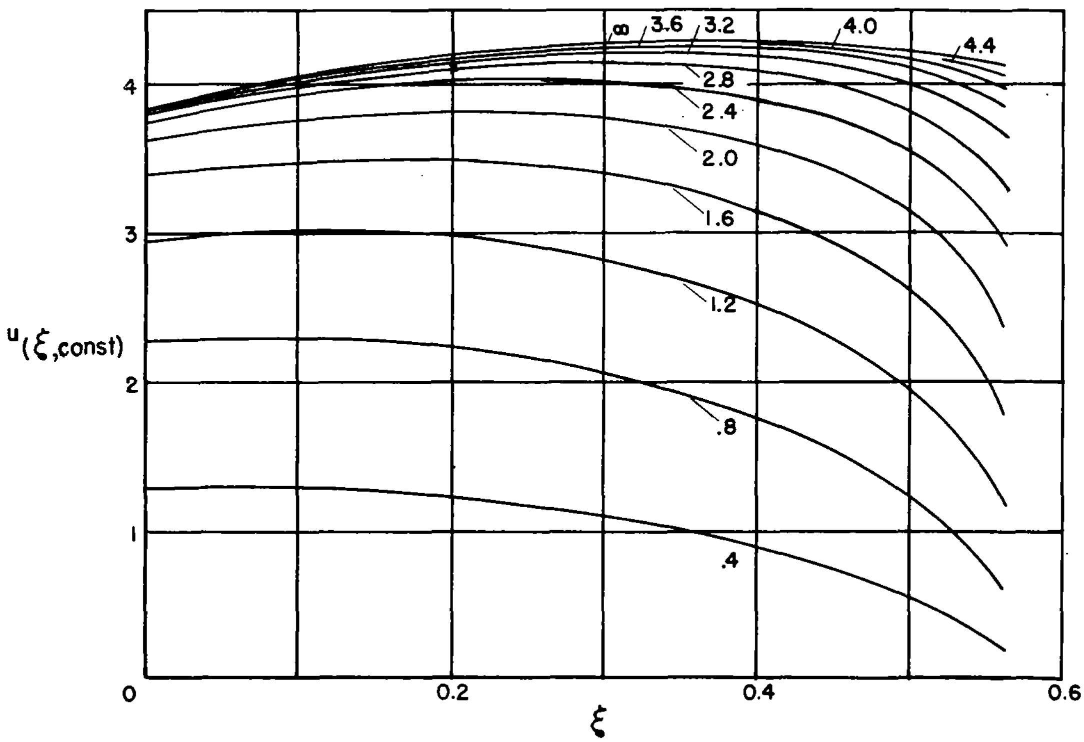

Figure 7.- The curves $u = u(\xi \text{ const.})$ for the circular cylinder.

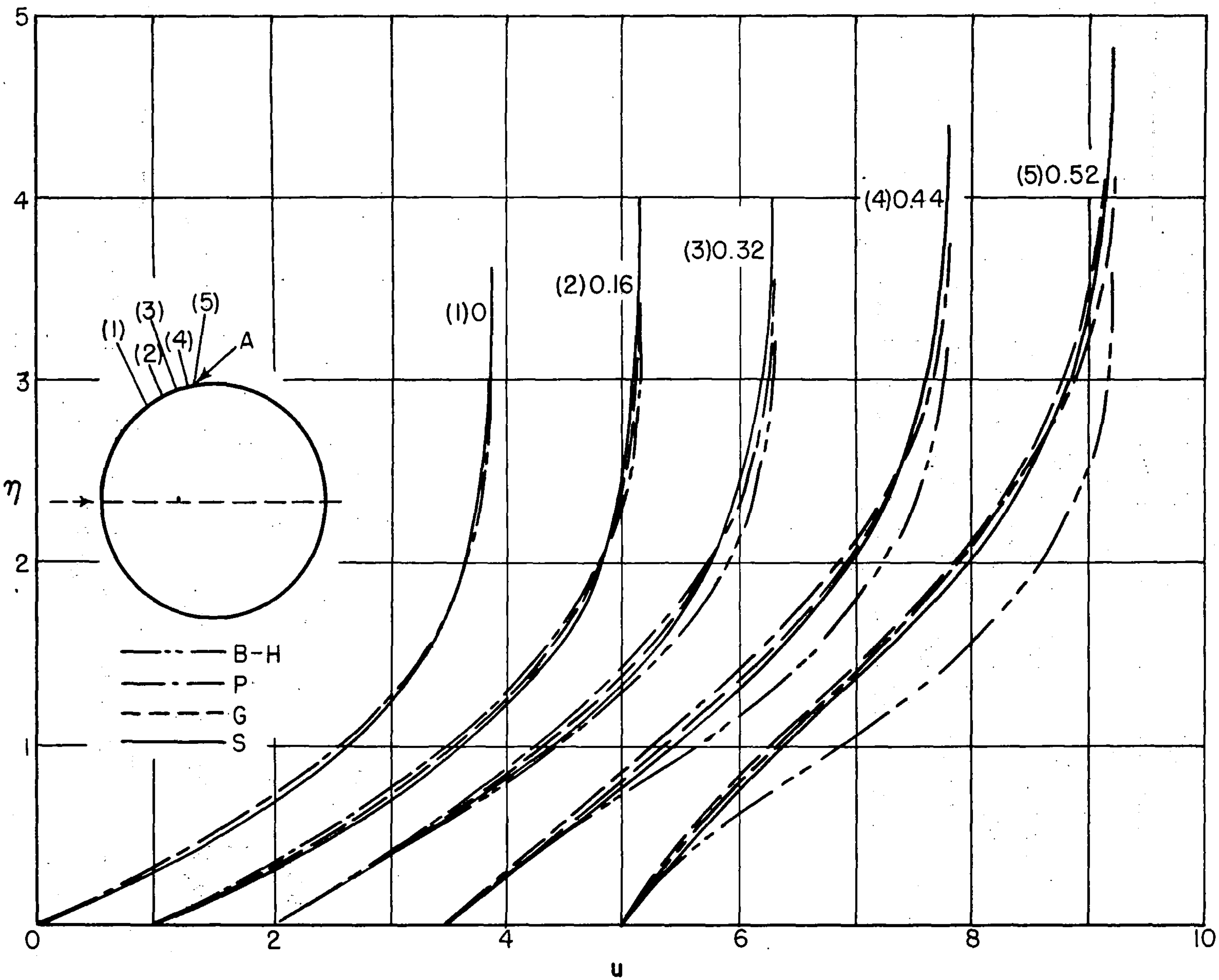

Figure 8.- Comparison of the profiles for the circular cylinder. For $\xi = 0.16$ the Blasius-Hiemenz profile coincides partly with Görtler's and partly with our profile.

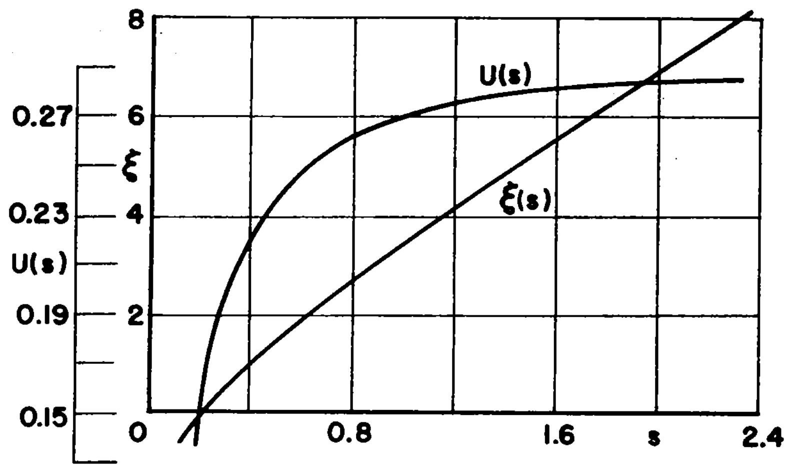

Figure 9(a).- The functions $\xi = \xi(s)$ and $U = U(s)$ for the elliptic cylinder.

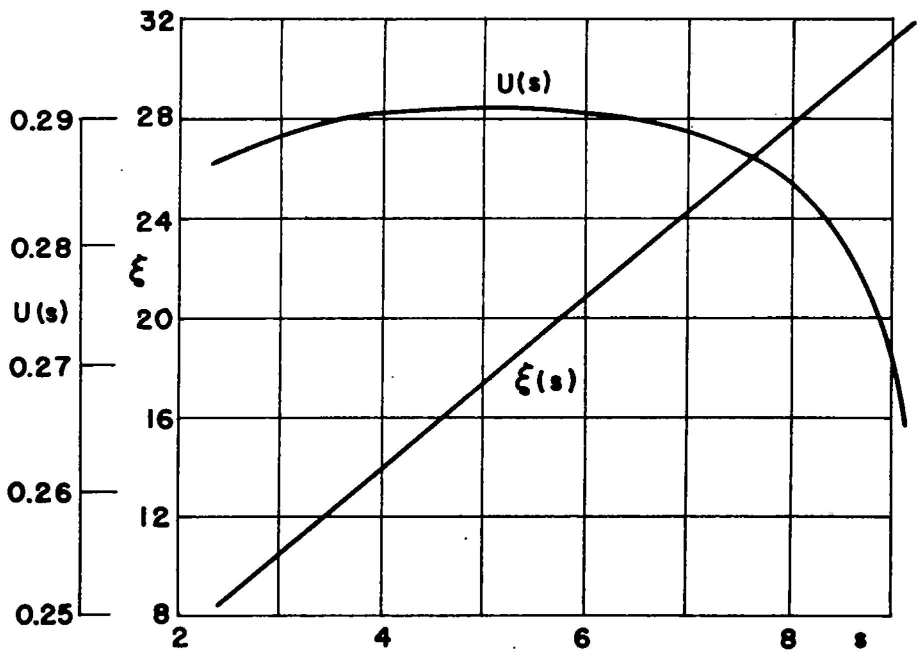

Figure 9(b).- The functions $\xi = \xi(s)$ and $U = U(s)$ for the elliptic cylinder.

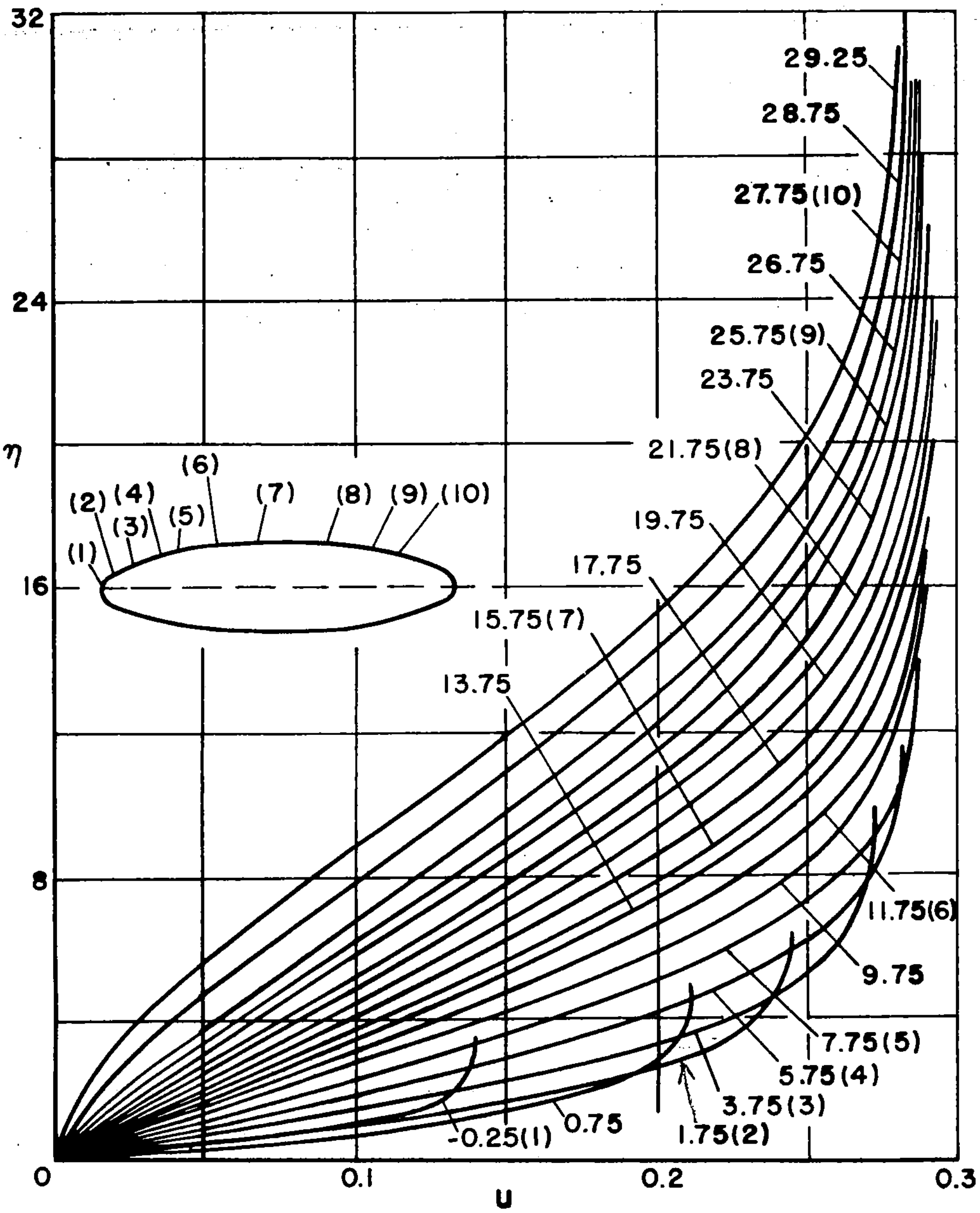

Figure 10.- Velocity profiles for the elliptic cylinder.

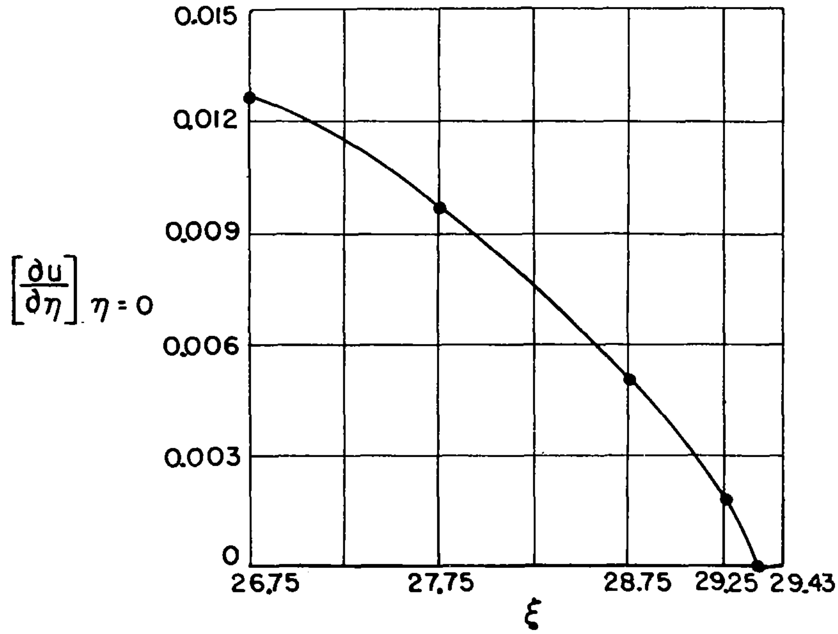

Figure 11.- Determination of the separation point for the elliptic cylinder.

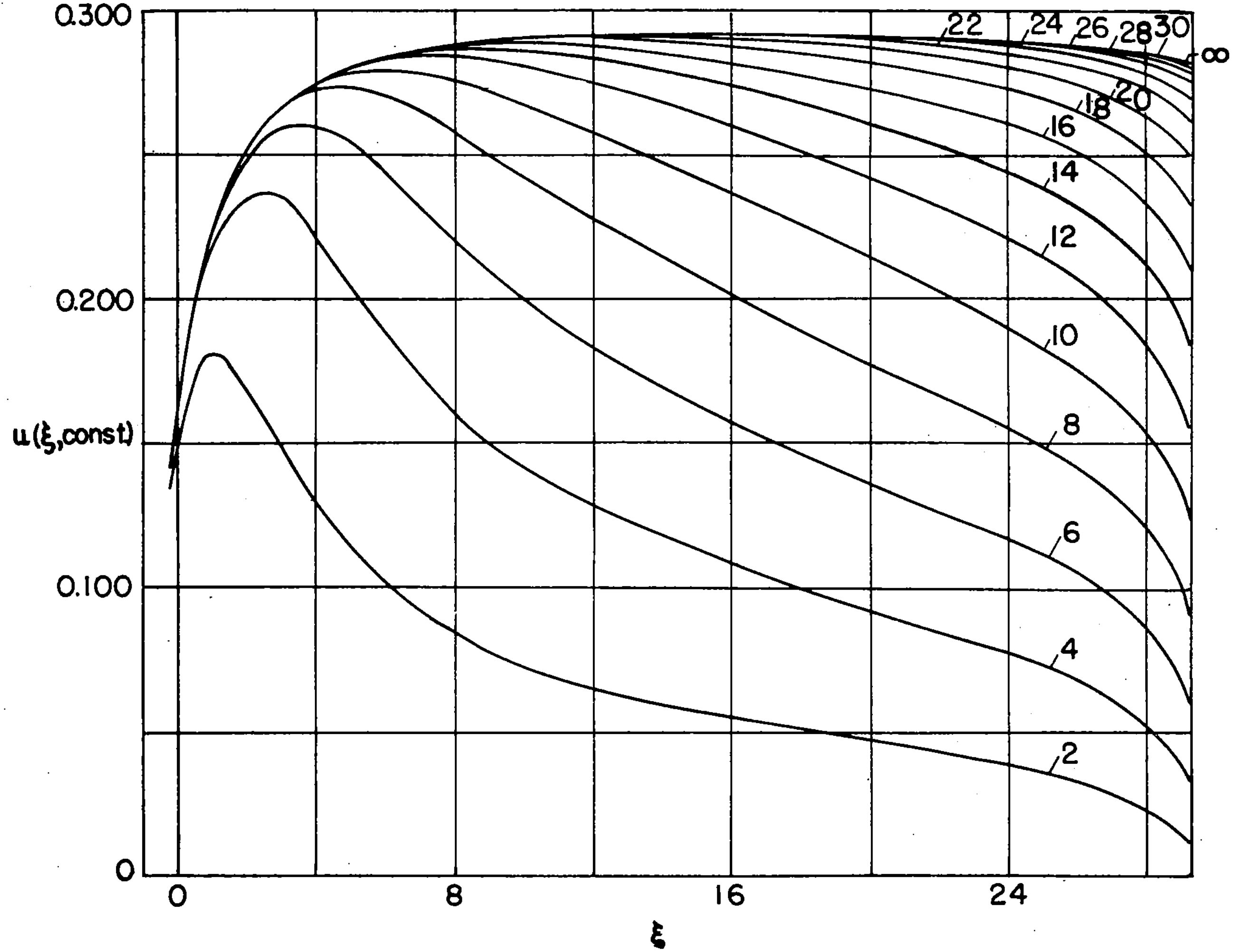

Figure 12.- The curves $u = u(\xi\ \text{const.})$ for the elliptic cylinder.

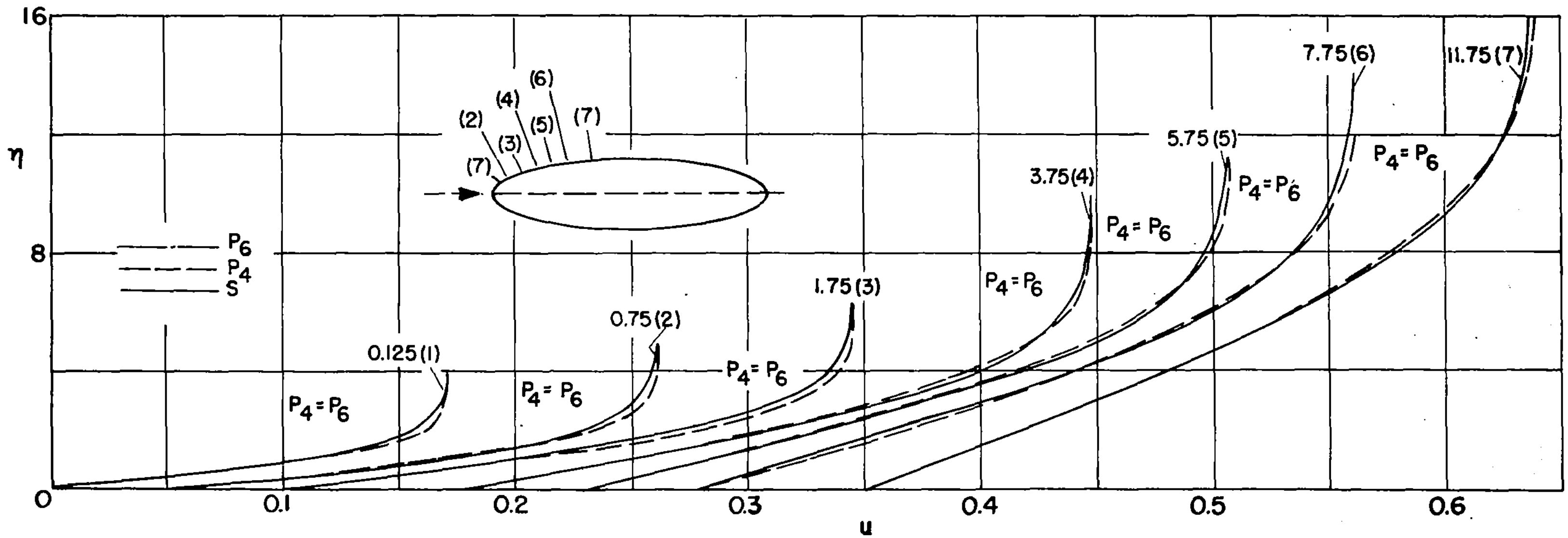

Figure 13.- Comparison of the profiles for the elliptic cylinder.

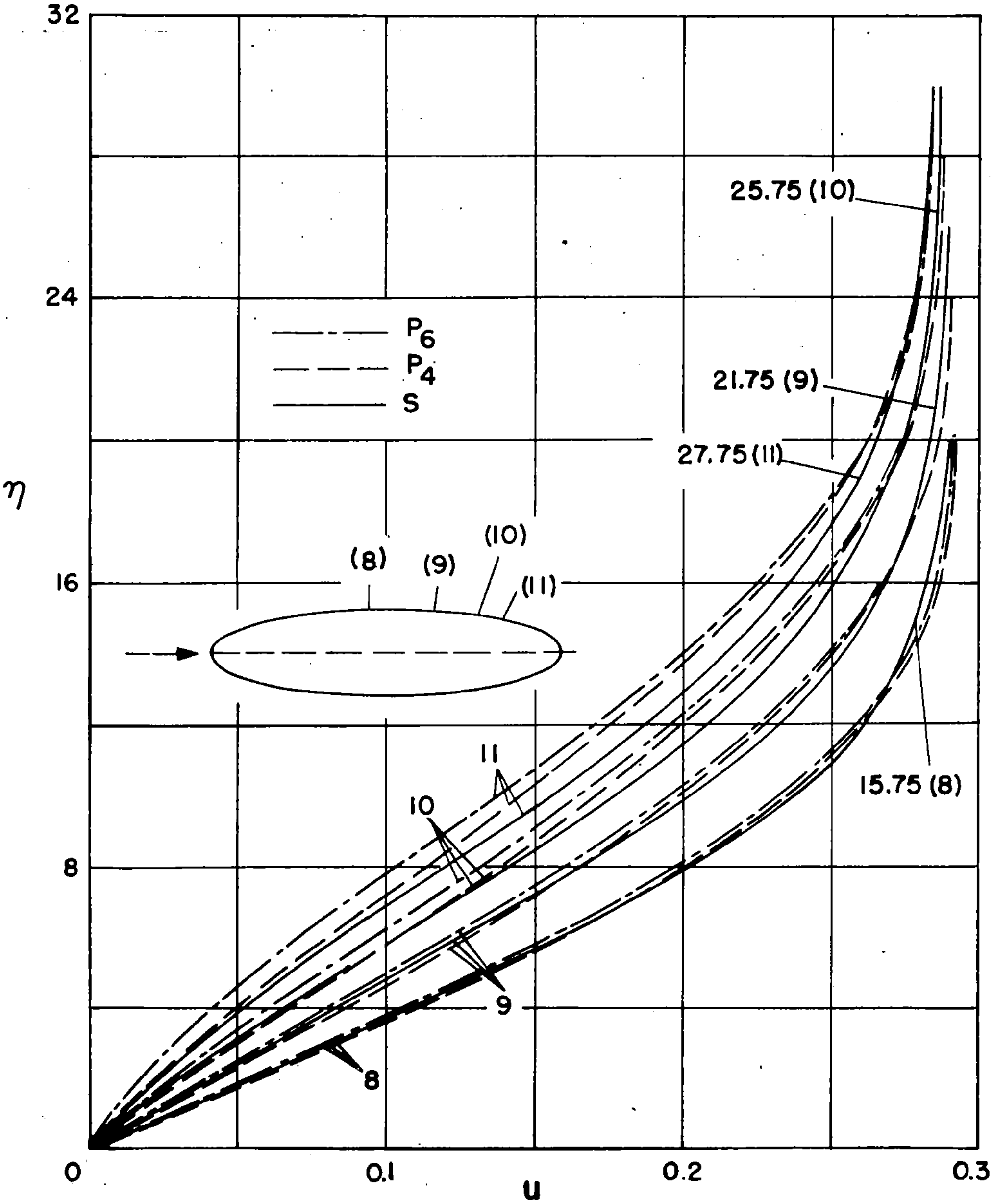

Figure 14.- Comparison of the profiles for the elliptic cylinder.